British Columbia carbonatites revisited: New whole rock Sr-Pb-Nd isotopic insights and drainage prospectivity trends

Alexei S. Rukhlov[1, a], Luke Ootes[1], Robert A. Creaser[2], Quinn F. Cunningham[1], Freia S. de Waal[1], and Devon K. Wenger[1]

[1] British Columbia Geological Survey, Ministry of Mining and Critical Minerals, Victoria, BC, V8W 9N3
[2] Department of Earth and Atmospheric Sciences, University of Alberta, Edmonton, AB, T6G 2E3
[a] corresponding author: Alexei.Rukhlov@gov.bc.ca

Recommended citation: Rukhlov, A.S., Ootes, L., Creaser, R.A., Cunningham, Q.F., de Waal, F.S., and Wenger, D.K., 2025. British Columbia carbonatites revisited: New whole rock Sr-Pb-Nd isotopic insights and drainage prospectivity trends. In: Geological Fieldwork 2024, British Columbia Ministry of Mining and Critical Minerals, British Columbia Geological Survey Paper 2025-01, pp. 119-139.

Abstract

Lithochemistry from modern drainages downstream of several known carbonatite and related alkaline-rock occurrences and a new calcite-dolomite carbonatite near Revelstoke reveals elevated (up to 100 times average continental crust) levels of rare earth elements (REE), Nb, Ta, and other carbonatite pathfinders. Panned, heavy mineral concentrate (HMC) samples show 10 times stronger contrast relative to bulk stream-sediment samples. Molybdenite from the past-producing Mount Copeland alkali syenite (ca. 740 Ma) yielded a Re-Os model age of 55.94 ±0.23 Ma, which ties the mineralization to a Paleogene metamorphic overprint. New whole rock Sr-Pb-Nd isotopic data from Neoproterozoic, Cambrian, and late Paleozoic carbonatites of the Blue River and Frenchman Cap areas, and Mount Copeland syenite record the evolution of a widespread, relatively primitive mantle source that was tapped episodically by carbonatites worldwide, at least since ca. 3 Ga, and by present-day ocean island basalts. The stream-sediment prospectivity criteria and carbonatite whole rock data compliment and link the sources of mineralization with host rocks and evolution of Cordilleran terranes. Our preliminary results inform the provincial assessment of carbonatite- and related-rock-hosted REE and rare metals through indicator minerals in archived Regional Geochemical Survey (RGS) samples.

Keywords: Carbonatite, alkaline rock, trace elements, Sr-Pb-Nd isotopes, Re-Os molybdenite, Mount Copeland, Blue River, stream sediment, heavy mineral concentrate (HMC), rare metals, rare earth elements (REE), mineral exploration

1. Introduction

Carbonatites, rare igneous rocks with at least 30% primary carbonate minerals, have become increasingly important exploration targets because they are major sources of Nb, rare earth elements (REE), and other metals on the critical mineral lists of many political jurisdictions (e.g., Hickin et al., 2024). In British Columbia, a belt of carbonatites straddles the western flank of Ancestral North America, some of which host REE and Nb-Ta mineralization (e.g., Mäder, 1987; Chudy, 2013; Ya'acoby, 2014; Chakhmouradian et al., 2015; Dalsin et al., 2015; Kulla and Hardy, 2015; Trofanenko et al., 2016; Rukhlov et al., 2018). Since the 1950s, sampling of modern drainage sediment across the province as part of the Regional Geochemical Survey (RGS) program has led to the discovery of precious and base metal deposits (Lett and Rukhlov, 2017; Rukhlov et al., 2024).

As part of a province-wide evaluation of carbonatite-hosted REE and rare-metals potential, this study presents preliminary lithochemical data from orientation sampling at several modern drainages downstream of known carbonatite and alkaline-rock occurrences in southeastern British Columbia (Fig. 1). The results from both panned, heavy-mineral concentrate (HMC) and bulk stream-sediment samples inform a regional assessment of carbonatite- and related rock-hosted mineralization through identifying carbonatite indicator minerals in archived samples (e.g., Belousova et al., 2002; Mackay and Simandl, 2015; Mao et al., 2016; Simandl et al., 2017). In addition, this study contributes to an ongoing British Columbia Geological Survey program that will generate hundreds of new whole rock radiogenic isotope (Sr-Pb-Nd-Hf) and trace-element analyses that will be reported in the future. Along with compiled analyses (Han et al., 2025), these data will help constrain the evolution of terranes and sources of mineralization and host rocks. We also contribute a new Re-Os model age on molybdenite from Mount Copeland historical mine and describe a previously unrecognized calcite-dolomite carbonatite occurrence at Boulder Mountain near Revelstoke.

2. British Columbia alkaline province

In British Columbia, carbonatites and silica-undersaturated and alkaline silicate rocks were emplaced episodically at ca. 810-690 Ma, 500-400 Ma, and 370-320 Ma forming part of the Cordilleran alkaline province (e.g., Pell, 1994; Millonig and Groat, 2013). This is a long (at least 1000 km), narrow (~200 km), orogen-parallel belt along the western flank of Laurentia (e.g., Okulitch et al., 1981; White, 1982; Mäder, 1987; Höy, 1988; Parrish and Scammell, 1988; Pell, 1994; Rukhlov and Bell, 2010; Millonig et al., 2012; Rukhlov et al., 2018).

Hosted by the parautochthonous rocks of the western

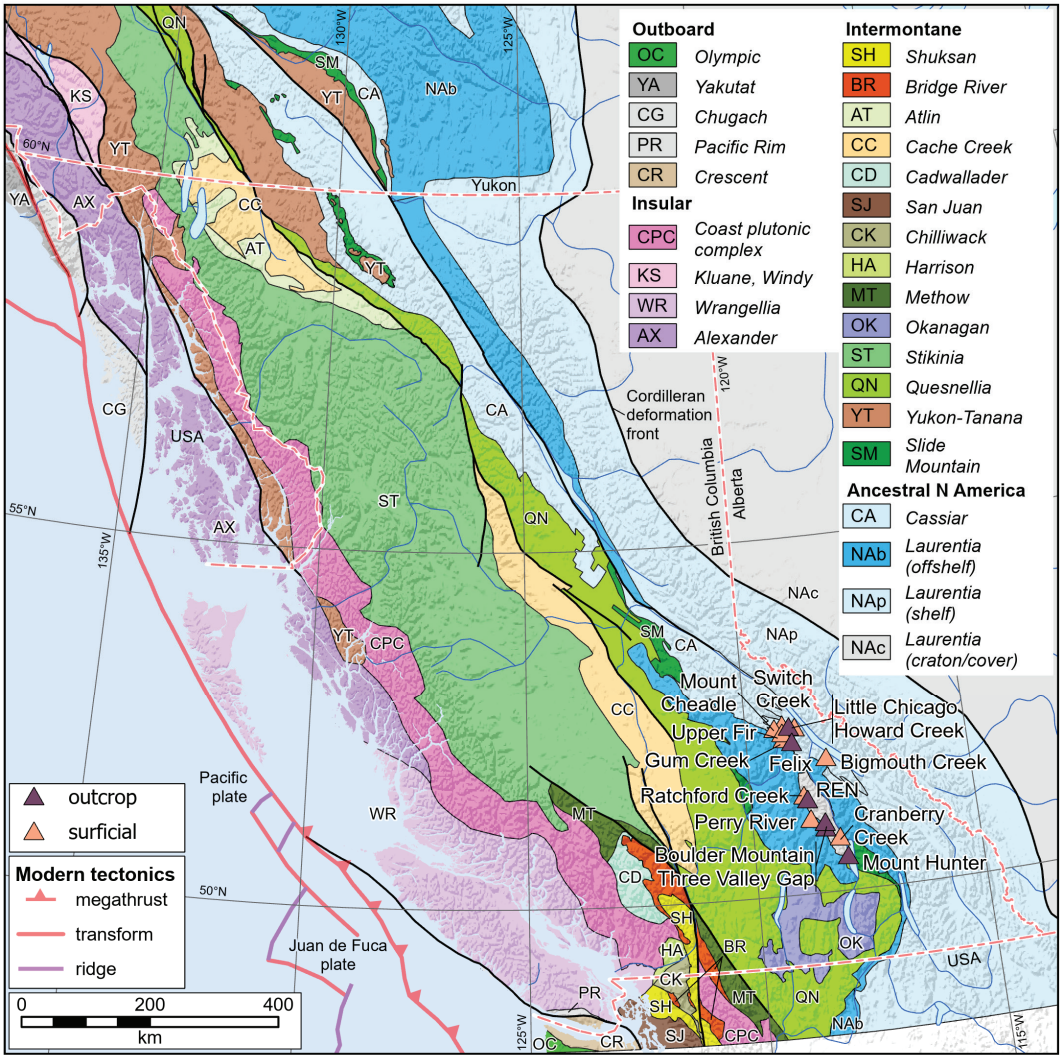

Fig. 1. Carbonatite localities and sampling sites, southeastern British Columbia. Terranes modified from Colpron (2020).

margin of Laurentia, carbonatites and related rocks range from intrusive complexes with a paucity of carbonatites (e.g., Trident Mountain, Mount Copeland) to carbonatite complexes with a paucity of silicate rocks (e.g., Blue River, Frenchman Cap). Both the carbonatites and host rocks experienced multiple episodes of deformation and metamorphism during Mesozoic and Cenozoic accretionary tectonics while outboard terranes welded to each other and to Laurentia (Scammell, 1987, 1993; Scammell and Brown, 1990; Pell, 1994; Millonig et al., 2013; Nelson et al., 2013). Some of these rocks host significant REE (e.g., Wicheeda; Dalsin et al., 2015; Trofanenko et al., 2016) and Ta-Nb (e.g., Aley; Mäder, 1987; Chakhmouradian et al., 2015; and Upper Fir; Chudy, 2013; Kulla and Hardy, 2015; Rukhlov et al., 2018).

3. Samples

This study contributes to province-wide geochemical re-analysis, including whole rock radiogenic isotope (Sr-Pb-Nd-Hf) and trace-element data from igneous rocks. We contribute new whole rock data from carbonatites and related alkaline rocks (7 localities, total 11 samples, including duplicates), and stream-sediment data (9 drainage sites, total 40 samples, including duplicates) downstream of known carbonatite or related-rock occurrences, or related geochemical anomalies (Fig. 1; Rukhlov et al., 2024). Rukhlov et al. (2025) provide complete analytical data sets and details of samples and methods used in this study.

3.1. Carbonatites and alkaline rocks

We sampled outcrops of ca. 500 Ma carbonatites (Felix and Little Chicago) in the Blue River area, east-central British Columbia (Figs. 2, 3), and both ca. 700 Ma (Ren or Ratchford Creek) and ca. 360 Ma (assumed emplacement age after Millonig et al., 2012; Three Valley Gap) carbonatites of the Monashee complex, southeastern British Columbia (e.g., Thompson et al., 2006). Detailed descriptions of the carbonatites can be found in Pell (1994), Millonig et al. (2012), Millonig and Groat (2013), and Rukhlov et al. (2018).

Fig. 2. Tectonically layered, light-toned dolomite-calcite carbonatite and dark-toned clinopyroxene-amphibole-phlogopite rock (fenite) crosscut by light-toned calcite veins; Little Chicago occurrence, Blue River area.

Fig. 3. Recrystallized carbonatite with layered, dark-toned porphyroclasts of magnetite and olivine set in a recrystallized dolomite-apatite-calcite matrix; Little Chicago occurrence, Blue River area.

Metamorphosed to amphibolite grade during Mesozoic to Cenozoic orogeny, carbonatites in the study area form isoclinally folded bodies with transposed layers that are rarely more than a few m thick (Fig. 2). These layers display diverse fabrics, including coarse-grained, granoblastic to fine-grained, foliated, and porphyroclastic varieties. Commonly heterogeneous on a cm-scale, they are made up of variable proportions of calcite, dolomite, fluorapatite, amphiboles, olivine, phlogopite, clinopyroxene, magnetite, ilmenite, and pyrrhotite (Figs. 4, 5). Accessory minerals include chondrodite, pyrite, molybdenite, pyrochlore supergroup, ferrocolumbite, fersmite, nyoboaeschynite, zircon, baddeleyite, zirconolite, and monazite (Millonig et al., 2012; Chudy, 2013; Rukhlov et al., 2018). Metasomatic glimmerites and calcite-clinopyroxene-amphibole-phlogopite rocks (i.e., fenites) mantle intrusive carbonatite bodies hosted by metamorphosed pelitic, arenaceous, calcareous, and amphibolitic rocks of the Mica Creek assemblage (Neoproterozoic) or Monashee complex (Proterozoic to Paleozoic).

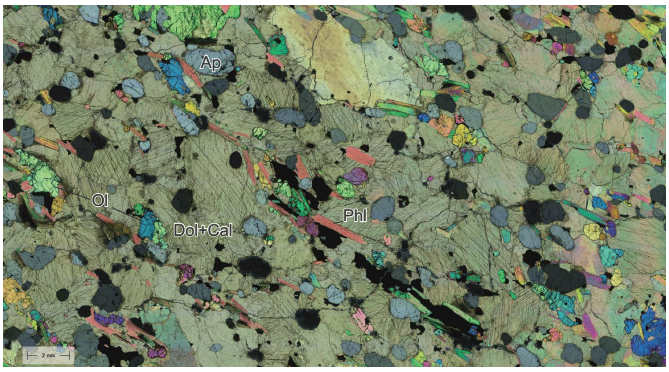

Fig. 4. Photomicrograph of recrystallized dolomite-calcite carbonatite in cross-polarized transmitted light with aligned, rounded apatite (Ap), fresh olivine (Ol), and phlogopite (Phl) set in a polygonal dolomite-calcite matrix with minor magnetite and pyrrhotite; Felix carbonatite, Blue River area.

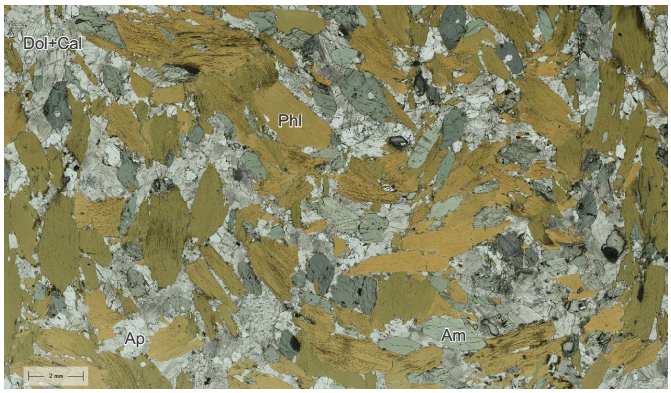

Fig. 5. Photomicrograph of phlogopite- and amphibole-rich, calcite-dolomite carbonatite in plane-polarized transmitted light with olive-brown phlogopite (Phl) and strongly pleochroic, light- to dark-toned greenish-grey amphibole (Am) set in recrystallized apatite (Ap)-calcite (Cal)-dolomite (Dol) matrix; Ren (Ratchford Creek) carbonatite, Frenchman Cap.

Based on new whole rock lithochemistry (Fig. 6), we have re-classified Mount Hunter 'extrusive carbonatite' in the Monashee complex (documented on Fig. 6 in Thompson et al., 2006) as marble (Rukhlov et al., 2025). In contrast, a ~1 m thick carbonate layer, traced for ~200 m along strike at Boulder Mountain in the Monashee complex near Revelstoke is a new carbonatite occurrence (Fig. 7). Hosted by grey marble and fenitized calc-silicate gneiss of the Monashee complex, the carbonatite is made up of coarse-grained dolomite and calcite, subordinate apatite, phlogopite, amphibole, and minor ilmenite and magnetite, and contains ~10% of fenitized feldspathic xenoliths (Fig. 8). Compositionally, the rock is within the range of carbonatites elsewhere in British Columbia (Fig. 6). Based on whole-rock Sr-Pb-Nd isotopic data discussed below, here we adopt an average age of ca. 360 Ma for most carbonatites in British Columbia (Millonig et al., 2012).

In addition, three samples of alkali syenite from Mount Copeland were retrieved from the BCGS rock archive for both whole rock analysis (samples 6550-E-1 and 6550-E-4) and Re-Os dating of molybdenite (sample 6550-E-3-2; Rukhlov et al., 2025). The molybdenite represents ore mineralization from the past-producing mine (Currie, 1976; Höy, 1988; Pell, 1994).

3.2. Drainage geochemical survey

We sampled modern drainage sediment downstream of several known carbonatite and alkaline-rock occurrences and related geochemical anomalies in the Blue River and Monashee complex areas (Figs. 9-15; Rukhlov et al., 2024). The area of the sampled catchment basins varies from ~0.5 km^2 to ~97 km^2. Both bulk stream-sediment and panned heavy mineral concentrate, sieved <0.18 mm and 0.18 to 1.0 mm fractions each, were analyzed for 65 analytes (Rukhlov et al., 2025). The lithochemical orientation survey informs the utility of indicator-mineral approach applied to archived, provincial drainage samples (Rukhlov et al., 2023). Mackay and Simandl (2015) and Simandl et al. (2017) developed a direct indicator approach based on identifying detrital Nb-Ta and REE ore minerals derived from carbonatites in stream sediments using an automated mineralogical analysis. However, many of these minerals are highly soluble and unlikely to survive fluvial transport. In contrast, both zircon and apatite are more chemically resistant and physically durable than some of the REE ore minerals (e.g., REE-F-carbonates). Thus, we also consider an indirect indicator mineral approach that uses chemical compositions of common detrital minerals such as zircon and apatite, which occur across the range of igneous and hydrothermal lithologies, as proxies of source rock type (e.g., Belousova et al., 2002; Mao et al., 2016). Below we summarize stream-sediment lithochemical results in terms of ranked element contrast relative to the average continental crust values of Rudnick and Gao (2014).

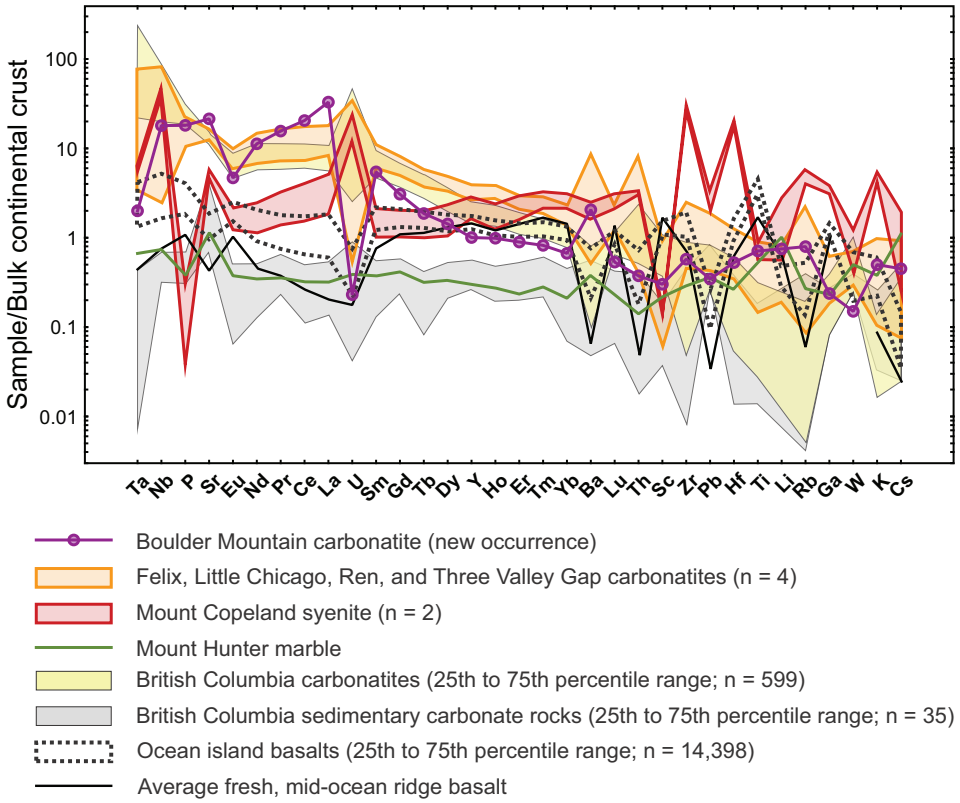

Fig. 6. Compositions of carbonatites, alkaline rocks, and sedimentary carbonate rocks in British Columbia normalized to the bulk continental crust values of Rudnick and Gao (2014); after Rukhlov et al. (2024, 2025). Average mid-ocean ridge basalt (MORB) after Kelemen et al. (2014). Compositional range for ocean island basalts (OIB) from GEOROC compilation (DIGIS Team, 2023).

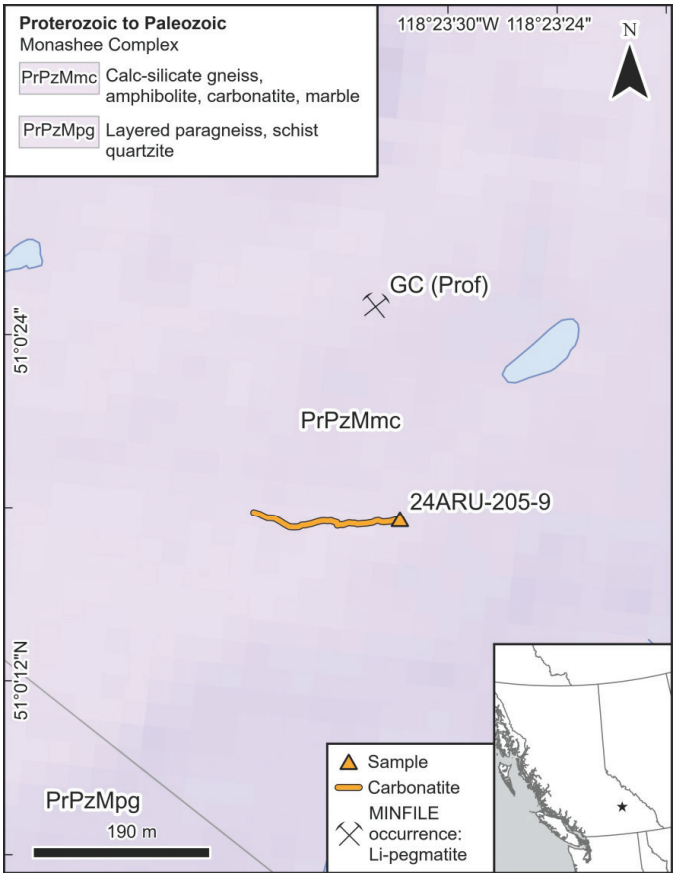

Fig. 7. Traced outcrop of ~1 m thick carbonatite layer at Boulder Mountain, Frenchman Cap complex, south-eastern British Columbia (82M/01). Geology after Rice and Jones (1960), Höy and Brown (1980), Johnson (1990), Logan (2002), and Cui et al. (2017).

Fig. 8. Calcite-dolomite carbonatite (oxidized brown) with dark-toned phlogopite and amphibole and light-toned feldspathic xenoliths in fenite layer; Boulder Mountain, southeastern British Columbia.

4. Dispersion of rare earth elements and rare metals in modern drainages

Based on the training of the RGS data using multivariate discriminant analysis, Rukhlov et al. (2024) ranked carbonatite-related geochemical signatures in terms of a 'carbonatite index' in bulk stream-sediment, <0.18 mm fraction, which is typically used in regional drainage geochemical surveys (Lett and Rukhlov, 2017). Normalized to continental crust values after Rudnick and Gao (2014) and arranged in order of contrast, the new stream-sediment data downstream of known carbonatite occurrences (Howard Creek, Gum Creek, Mount Cheadle, Ren, and Switch Creek) reveal up to two orders of magnitude contrast, including up to 3.70 wt% P, 1.61 wt.% ∑REE (i.e., La + Ce + Pr + Nd + Sm + Eu + Gd + Tb + Dy + Ho + Er + Tm + Yb + Lu), 0.40 wt.% Nb, 940 ppm Th, 229 ppm U, and 190 ppm Ta (Figs. 10-12, 14; Rukhlov et al., 2025). The response from the Trident Mountain alkaline complex (ca. 359 Ma. Millonig et al., 2012), which hosts both REE and rare-metal mineralization (Brown, 2012), is indistinguishable from that of carbonatites (Fig. 9). Resampling of high-ranked, carbonatite-related drainage anomalies at both Perry River and Cranberry Creek (Rukhlov et al., 2024), confirms the multi-element carbonatite or related-rock signal from these catchment basins, thereby underscoring their prospectivity for REE mineralization (Figs. 13, 15).

Because REE, Nb, Ta and other carbonatite indicator elements are mainly concentrated in relatively high-density minerals such as pyrochlore supergroup, ferrocolumbite, fersmite, nyoboaeschynite, Nb-ilmenite, zirconolite, euxenite, allanite, monazite, apatite, and REE-F-carbonates (Chudy, 2013; Chakhmouradian et al., 2015; Mackay and Simandl, 2015; Rukhlov et al., 2018; Gammons et al., 2024), panned heavy mineral concentrates invariably show much stronger contrast relative to bulk stream sediment and thus is the preferred sample medium in REE-Nb prospecting (Rukhlov et al., 2024). In contrast, although generally at background levels, Ba, Cs, K, and Rb abundances are higher in bulk stream sediment relative to heavy mineral concentrates, perhaps reflecting low-density hosts such as mica and feldspar. Based on compiled data from Blue River area (Rukhlov et al., 2024), background concentrations of carbonatite pathfinders such as rare metals and REE in panned heavy mineral concentrate samples from carbonatite-free catchments are generally at the level of those in bulk stream-sediment (RGS) samples. Strontium, which is typically at least 10 times more abundant in carbonatites relative to the crust (Fig. 6), is at background levels in stream sediments (Figs. 9-15), which suggests mainly non-mechanical dispersion due to readily weathered carbonate hosts (Fig. 8). Differences in relative abundances of certain elements between the fine (<0.18 mm) and coarse (0.18 to 1.0 mm) fractions reflect both the mineralization (i.e. fine- versus coarse-grained) and distance of transport in the dispersion stream.

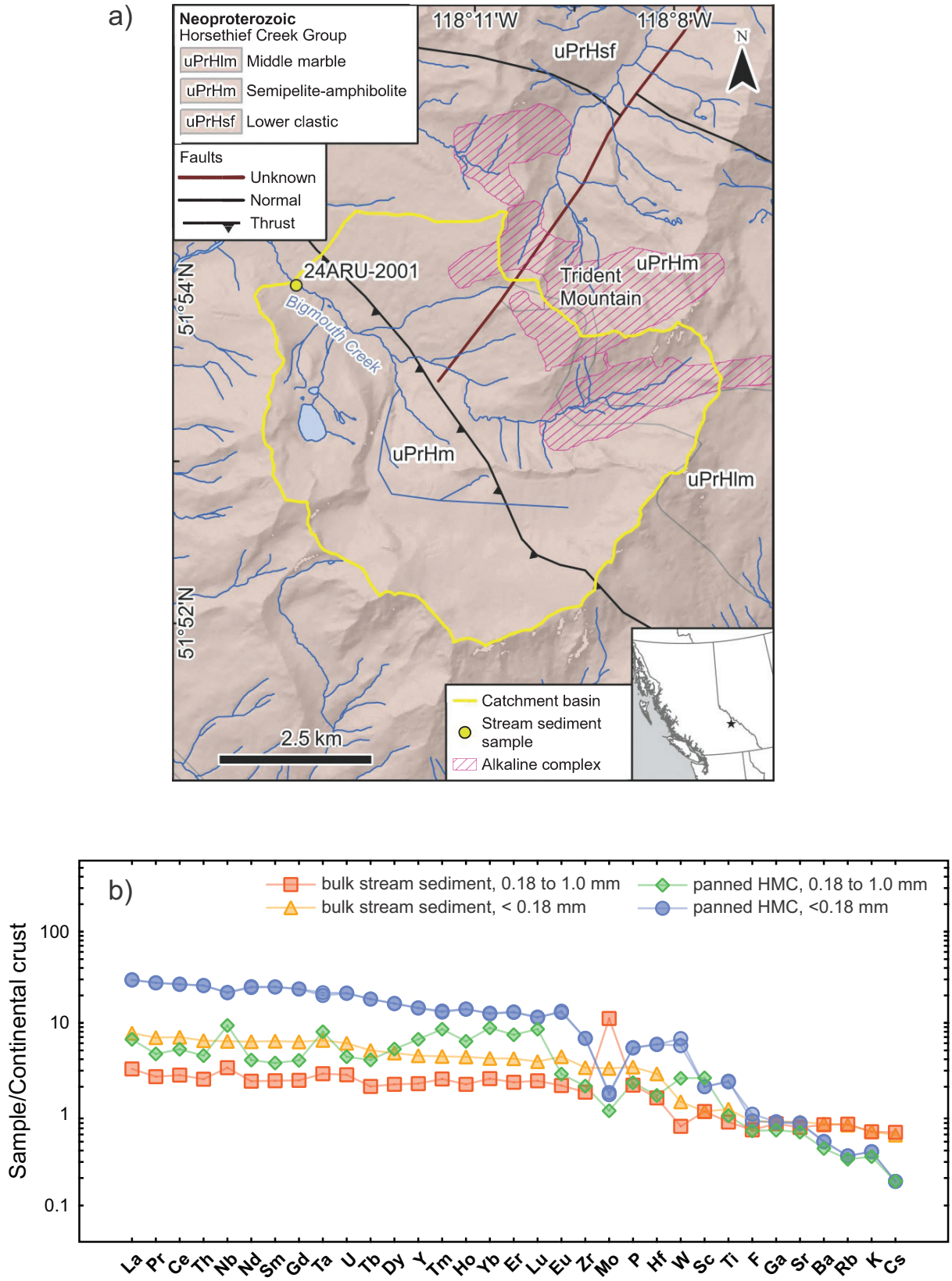

Fig. 9. a) Sampling site and catchment basin (area=34.21 km^2) at Bigmouth Creek, downstream of the Trident Mountain alkaline complex (082M/16; Pell et al., 1994). Trident Mountain alkaline complex footprint after Brown (2012). Geology after Wheeler and Fox (1964), Logan (2002), and Cui et al. (2017). **b)** Bulk stream-sediment and panned, heavy mineral concentrate (HMC) data normalized to bulk continental crust values of Rudnick and Gao (2014).

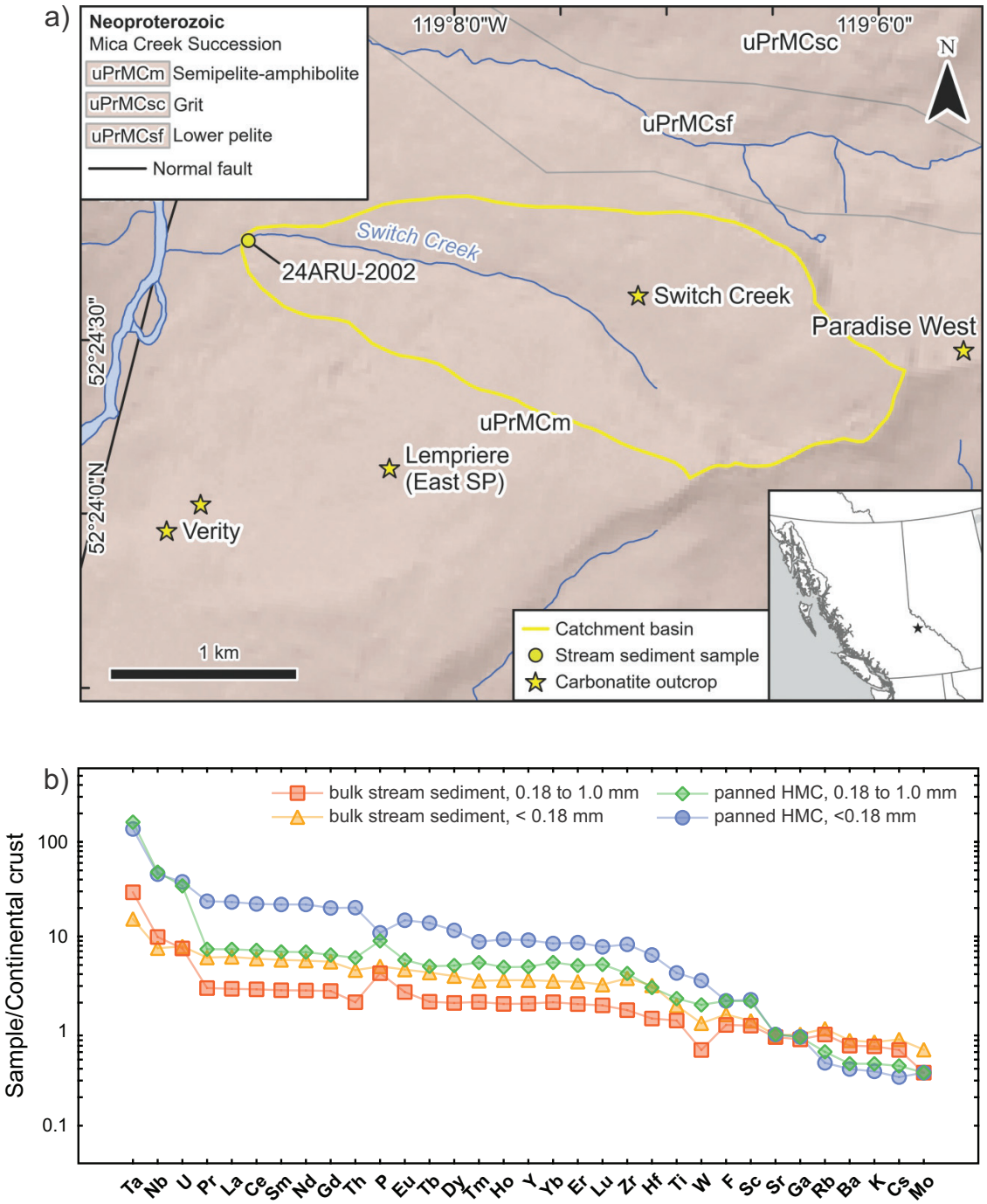

Fig. 10. a) Sampling site and catchment basin (area=3.17 km^2) at Switch Creek, downstream of Switch Creek carbonatite, Blue River area (83D/06). Carbonatite occurrences after Rukhlov et al. (2018). Geology after Campbell (1968), Simony et al. (1980), Raeside and Simony (1983), Pell and Simony (1987), McDonough et al. (1991, 1992), Murphy (2007), and Cui et al. (2017). **b)** Bulk stream-sediment and panned, heavy mineral concentrate (HMC) data normalized to bulk continental crust values of Rudnick and Gao (2014).

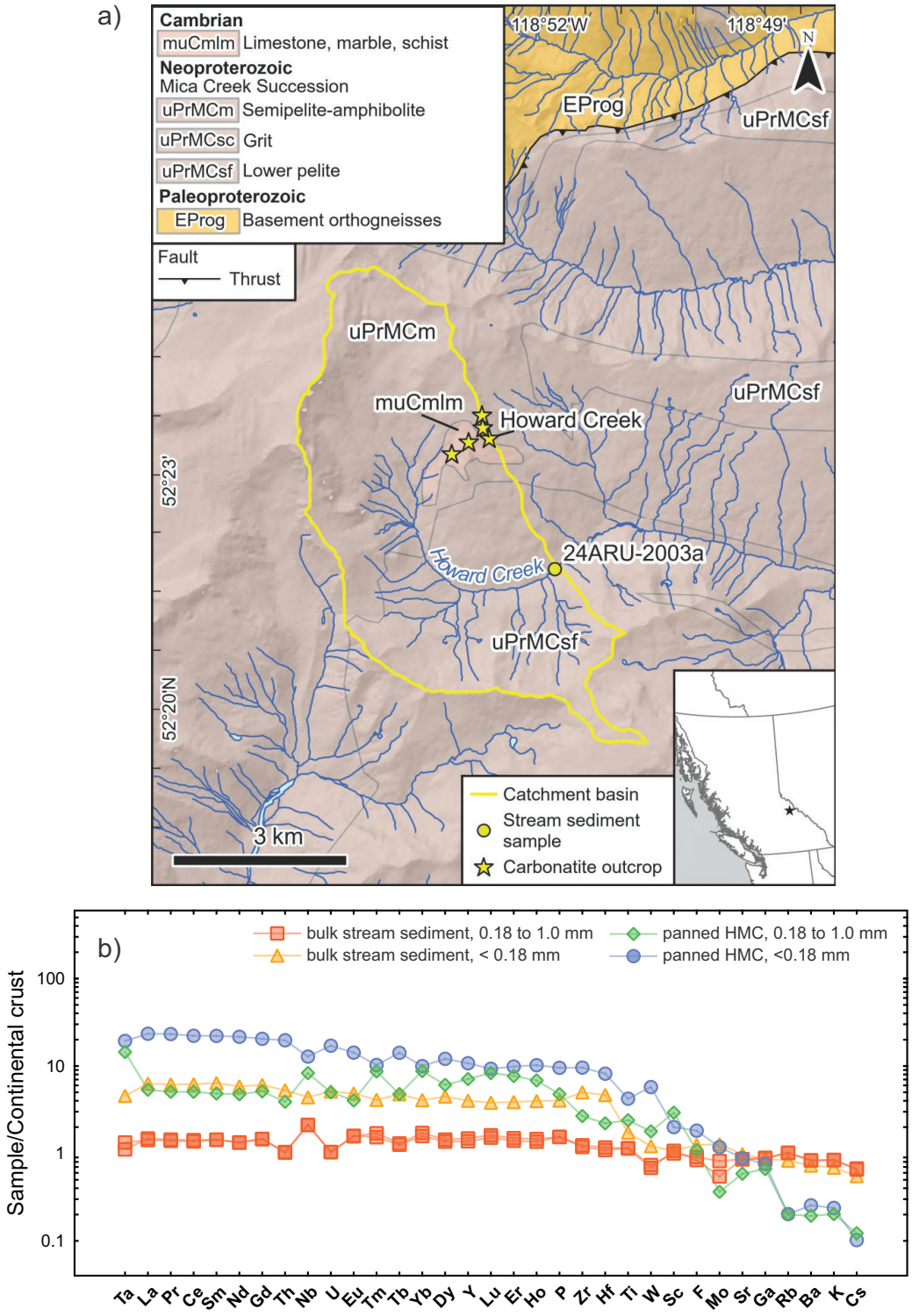

Fig. 11. a) Sampling site and catchment basin (area=28.60 km^2) at Howard Creek, downstream of Howard Creek carbonatites, Blue River area (83D/07). Carbonatite occurrences after Rukhlov et al. (2018). Geology after Campbell (1968), Simony et al. (1980), Raeside and Simony (1983), Pell and Simony (1987), McDonough et al. (1991, 1992), Murphy (2007), and Cui et al., (2017). **b)** Bulk stream-sediment and panned, heavy mineral concentrate (HMC) data normalized to bulk continental crust values of Rudnick and Gao (2014).

5. Re-Os molybdenite model age

Molybdenite occurs sporadically in carbonatites and related rocks of the Cordilleran alkaline province, including the Mount Copeland historical molybdenum producer, and alkali-rich, metasomatic fenites and glimmerites that mantle carbonatite bodies (Currie, 1976; White, 1982; Höy, 1988; Trofanenko et al., 2016; Rukhlov et al., 2018; Gammons et al., 2024). In contrast, carbonatites in typical anorogenic settings are generally poor in Mo (average 12 ppm) and lack molybdenite (Woolley and Kempe, 1989). With Mo production from a unique carbonatite-hosted deposit at Huanglongpu in central China (Quinling orogenic belt), evidence is growing that carbonatite magmatism in atypical tectonic settings such as cratonic margins or orogenic belts can generate economic Mo deposits (Xu et al., 2010; Song et al., 2016).

To constrain the timing of Mo mineralization, we analyzed molybdenite from the Mount Copeland alkaline complex for Re-Os (see Rukhlov et al., 2025 for details). The sample (6550-E-3-2) represents ore from the past-producing mine (Currie, 1976; Höy, 1988; Pell, 1994) and was retrieved from the BCGS rock archive. The molybdenite returned a Re-Os model age of 55.94 ±0.23 (2σ) Ma, broadly consistent with the U-Pb dates of 59 ±1 Ma on metamorphic zircons (Okulitch et al., 1981; Parrish and Scammell, 1988). The imprecise U-Pb zircon date of 740 ±36 Ma, interpreted as crystallization age of the host syenite at Mount Copeland (Okulitch et al., 1981; Parrish and Scammell, 1988), agrees with more precise LA-ICP-MS U-Pb zircon dates of 793.5 ±7.6 Ma and 797.5 ±6.5 Ma from other alkaline syenites in the Frenchman Cap area (Millonig et al., 2012). Therefore, our Re-Os molybdenite model age of ca. 56 Ma constrains the Mo mineralization at Mount Copeland to coincide with a Paleogene metamorphic overprint (Parrish, 1995; Crowley and Parrish, 1999; Millonig et al., 2012, 2013). Rukhlov et al. (2018) reported Re-Os model age of 175.3 ±0.8 (2σ) Ma for coarse (up to 1.7 cm long) molybdenite from the Upper Fir carbonatite (ca. 330 Ma) in the Blue River area (Fig. 12a). The molybdenite has 22.75 ±0.07 (2σ) ppm total Re, 14.30 ±0.04 (2σ) ppm ^{187}Re, and 41.81 ±0.03 (2σ) ppb ^{187}Os, and lacks common Os above blank level. Because replicate analysis of the same molybdenite mineral separate yielded a distinct Re-Os model age of 198.5 ±0.9 (2σ) Ma, the molybdenite is strongly decoupled with respect to Re and Os, suggesting a Jurassic metamorphic overprint (Rukhlov et al., 2018), also documented by Millonig et al. (2012) in U-Pb zircon results from the Little Chicago carbonatite.

6. Trace-element and Sr-Pb-Nd isotopic constraints on the source of carbonatite-hosted rare metals

Carbonatite whole rock data provide the link between stream-sediment data and the sources of mineralization and provide information on host rocks and terrane evolution. In addition to distinct physical and mineralogical characteristics, which can be difficult to recognize in the field, most carbonatites are readily distinguished from recrystallized sedimentary carbonate rocks by their extremely high concentrations (up to 100 times that of the average continental crust) of Ta, Nb, P, Sr, REE, Ba, and other elements (Fig. 6; Woolley and Kempe, 1989). Mount Copeland alkali syenites show similar levels of Ba, Nb, Ta, Th, and U, but much higher Ga, Hf, K, Rb, and Zr, and lower P, Sr, and REE abundances relative to the carbonatites (Fig. 6). The unusual geochemical characteristics of carbonatites are generally attributed to their origin as low-degree partial melts of carbonate-bearing mantle below 75 km, or as products of immiscible separation or fractional crystallization of parental carbonated silicate magmas (see reviews in Bell, 1989; Bell et al., 1998; Bell and Rukhlov, 2004; Yaxley et al., 2021; Schmidt et al., 2024). Buffered from crustal contamination by the extreme Sr and Nd concentrations, ^{87}Sr/^{86}Sr and ^{143}Nd/^{144}Nd ratios in carbonatites provide robust insights into the sub-continental mantle. Below we summarize the new Sr-Pb-Nd data and those compiled in Han et al. (2025) from British Columbia carbonatites and related rocks in the framework of data from globally distributed carbonatites, which span ages from ca. 3.0 Ga to the present (Figs. 16-18; Rukhlov et al., 2015 and references therein).

Initial ^{87}Sr/^{86}Sr (0.703108 to 0.705076) and initial ^{143}Nd/^{144}Nd (0.511749 to 0.512433; Rukhlov et al., 2025) are recast as $\varepsilon_{Sr}(T)$ and $\varepsilon_{Nd}(T)$ notations, respectively (Fig. 16), which are the relative differences in parts per 10^4 (ε, epsilon) between a sample and a reference such as bulk Earth for Sr (DePaolo and Wasserburg, 1976; DePaolo, 1988) and chondritic uniform reservoir (CHUR) for Nd (Jacobsen and Wasserburg, 1980; Hamilton et al., 1983). Isotope development diagrams (Fig. 16) in terms of time versus $\varepsilon_{Sr}(T)$ and $\varepsilon_{Nd}(T)$ for ca. 0.80-0.69 Ga, ca. 0.50 Ga, and ca. 0.37-0.32 Ga carbonatites in British Columbia reveal evolution of a heterogeneous, generally depleted (i.e. super-chondritic and sub-bulk Earth) mantle source consistent with that tapped by carbonatites elsewhere for the last 3 billion years (Rukhlov et al., 2015).

Whole-rock initial ^{206}Pb/^{204}Pb (14.07-24.95), initial ^{207}Pb/^{204}Pb (15.21-15.96), and initial ^{208}Pb/^{204}Pb (36.94-40.51) ratios (Rukhlov et al., 2025) partly overlap Pb compositions from Cordilleran carbonatites and related rocks and those from ca. 0.37 Ga Kola alkaline province (Fig. 17; Rukhlov et al., 2015; Han et al., 2025; and references therein). The Pb isotopic compositions of whole-rock and mineral fractions (including galena) from carbonatites generally record evolution of a lower ^{238}U/^{204}Pb and higher ^{232}Th/^{204}Pb source than the second-stage Pb growth curve of Stacey and Kramers (1975), but more radiogenic relative to depleted mantle model using present-day ^{206}Pb/^{204}Pb, ^{207}Pb/^{204}Pb, and ^{208}Pb/^{204}Pb values of Rehkämper and Hofmann (1997) (Fig. 17). Whole rock data from Little Chicago and Three Valley Gap carbonatites (Rukhlov et al., 2025), and some carbonate, apatite, and molybdenite fractions from carbonatites of the Blue River and Frenchman Cap areas have extremely radiogenic (high) initial Pb isotopic ratios (Fig. 17 insets; Rukhlov et al., 2018; Han et al., 2025 and references therein). In contrast, the whole rock initial ^{206}Pb/^{204}Pb and initial

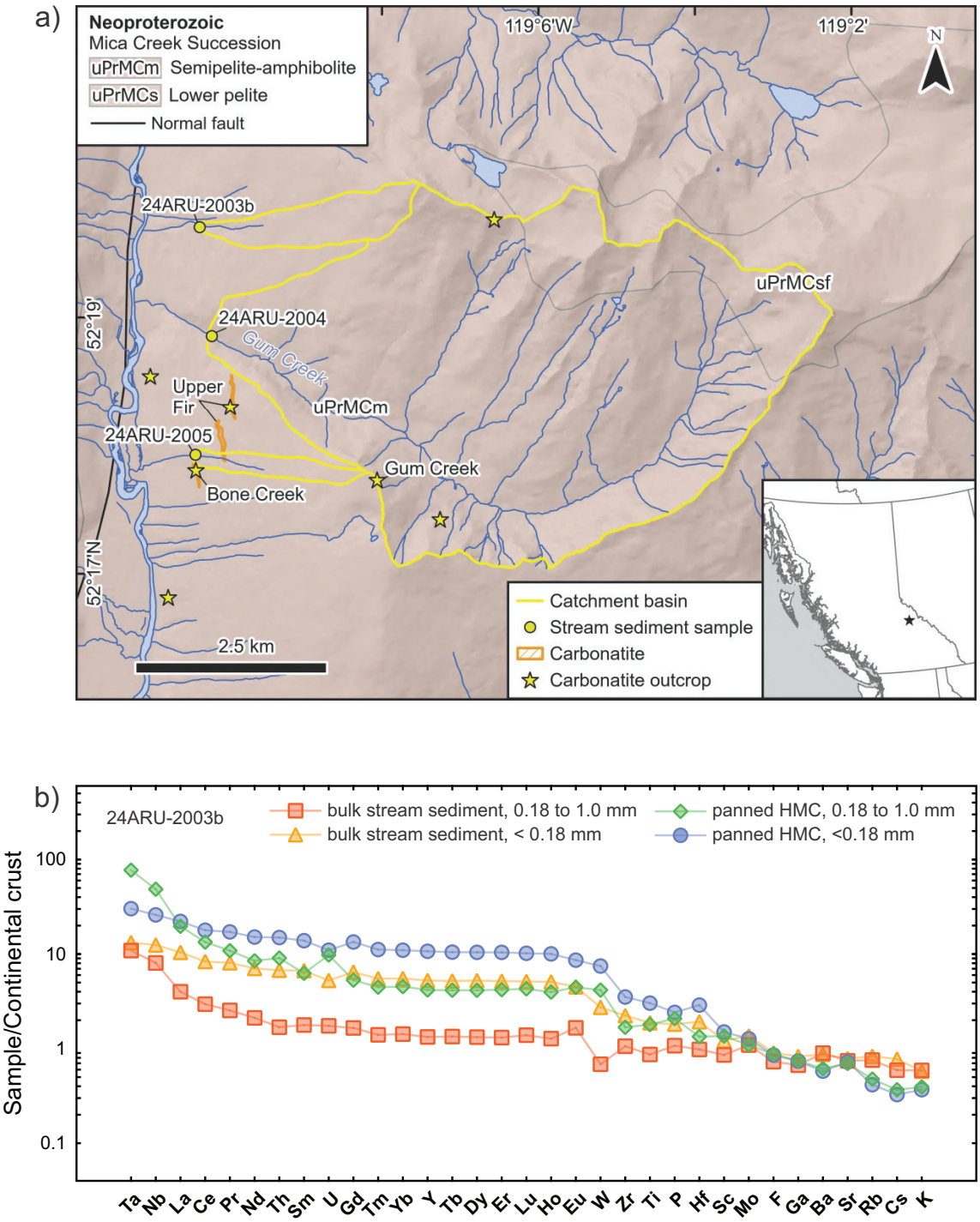

Fig. 12. a) Sampling sites and catchment basins downstream of carbonatites in the Blue River area (083D/06): Mount Cheadle (24ARU-2003b; catchment area=1.33 km^2), Gum Creek (24ARU-2004; catchment area=25.28 km^2), and Upper Fir (24ARU-2005; catchment area=0.52 km^2). Carbonatite occurrences after Rukhlov et al. (2018). Geology after Campbell (1968), Simony et al. (1980), Raeside and Simony (1983), Pell and Simony (1987), McDonough et al. (1991, 1992), Murphy (2007), and Cui et al. (2017). **b)** Bulk stream-sediment and panned, heavy mineral concentrate (HMC) data for 24ARU-2003b, normalized to bulk continental crust values of Rudnick and Gao (2014).

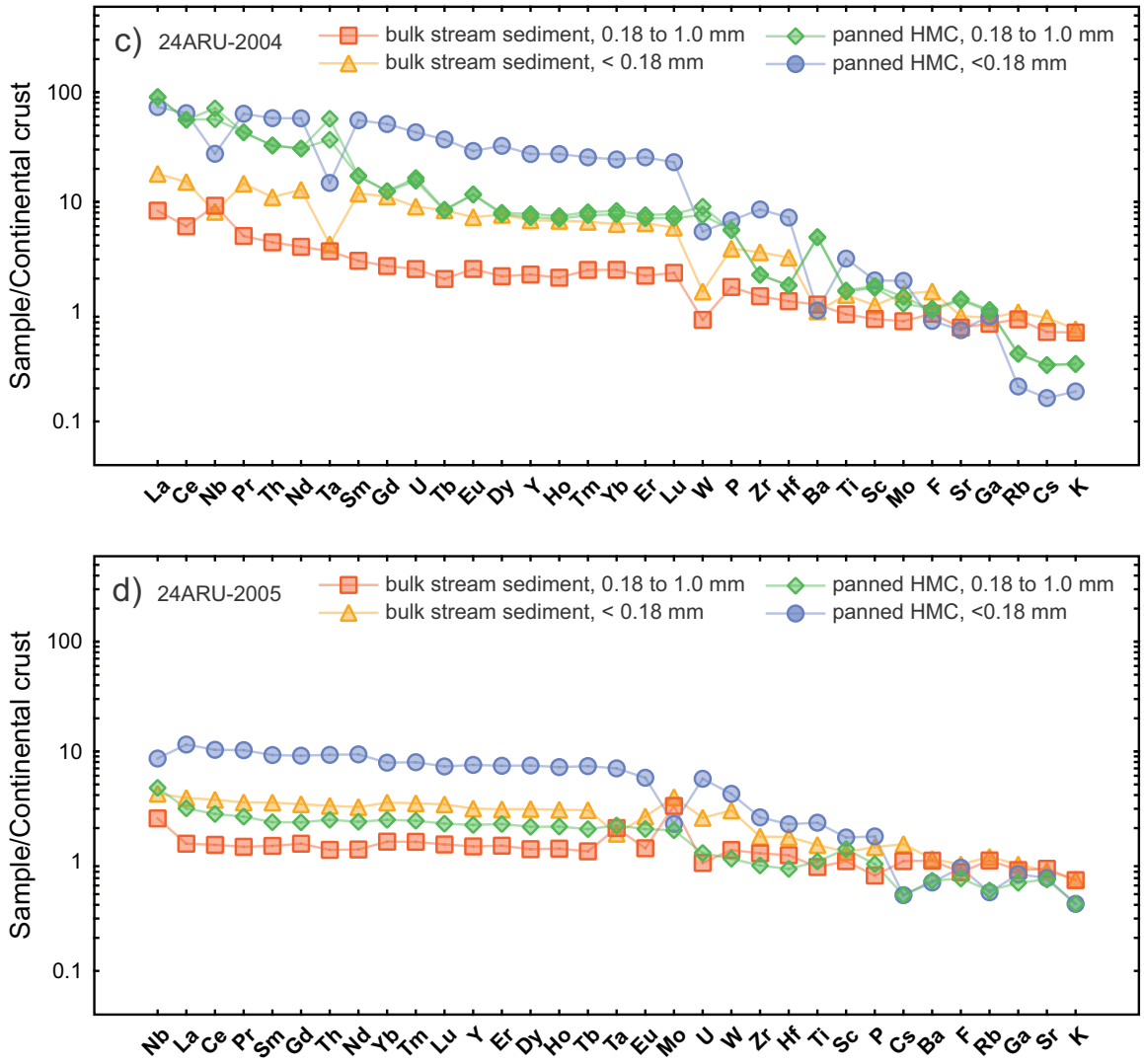

Fig. 12. Continued. **c)** Bulk stream-sediment and panned, heavy mineral concentrate (HMC) data for 24ARU-2004, normalized to bulk continental crust values of Rudnick and Gao (2014). **d)** Bulk stream-sediment and panned, heavy mineral concentrate (HMC) data for 24ARU-2005, normalized to bulk continental crust values of Rudnick and Gao (2014).

$^{207}Pb/^{204}Pb$ ratios from ca. 740 Ga Mount Copeland are too low (Fig. 17a; Rukhlov et al., 2025), probably reflecting U-Pb disturbance due to the Paleogene overprint as indicated by the ca. 56 Ma Re-Os model age on molybdenite. The disturbed U-Pb data from Mount Copeland are excluded from the following discussion. On the other hand, the initial $^{208}Pb/^{204}Pb$ ratios from Mount Copeland are consistent with those from carbonatites and related rocks in British Columbia (Fig. 17b; Han et al., 2025 and references therein). This suggests that the Th-Pb was relatively unaffected by the overprint that disturbed U-Pb at Mount Copeland.

Çimen et al. (2019) suggested a widespread, extremely radiogenic Pb mantle reservoir for the source of carbonatites from Blue River, Fen (Norway), Shaxiongdong, and Miaoya (China). However, Fen is the only anorogenic example in their comparison, and the data are not initial isotopic ratios (Andersen and Taylor, 1988). Carbonatites from anorogenic settings lack such extremely high initial Pb isotopic compositions (Fig. 17; Rukhlov et al., 2015 and references therein). The examples from China and British Columbia are metacarbonatites within orogenic belts (Chen et al., 2018; Çimen et al., 2018, 2019; Rukhlov et al., 2018; Han et al., 2025) and Rukhlov et al. (2018) attributed the signatures in Blue River to Pb-loss from U-rich pyrochlore, and its concurrent sequestering into co-existing minerals such as apatite, carbonates, and molybdenite during metamorphism. Data from these minerals define a linear array in the initial $^{206}Pb/^{204}Pb$ vs. initial $^{207}Pb/^{204}Pb$ diagram (Fig. 17a inset; Han et al., 2025), yielding a Pb-Pb isochron date (using robust regression) of 324 ±40 Ma (95% confidence) consistent with the emplacement ages of most carbonatites in the Blue River area (Rukhlov et al., 2018). British Columbia carbonatites with the least radiogenic Pb compositions are consistent with those from typical anorogenic examples, including Kola alkaline province (Fig. 17).

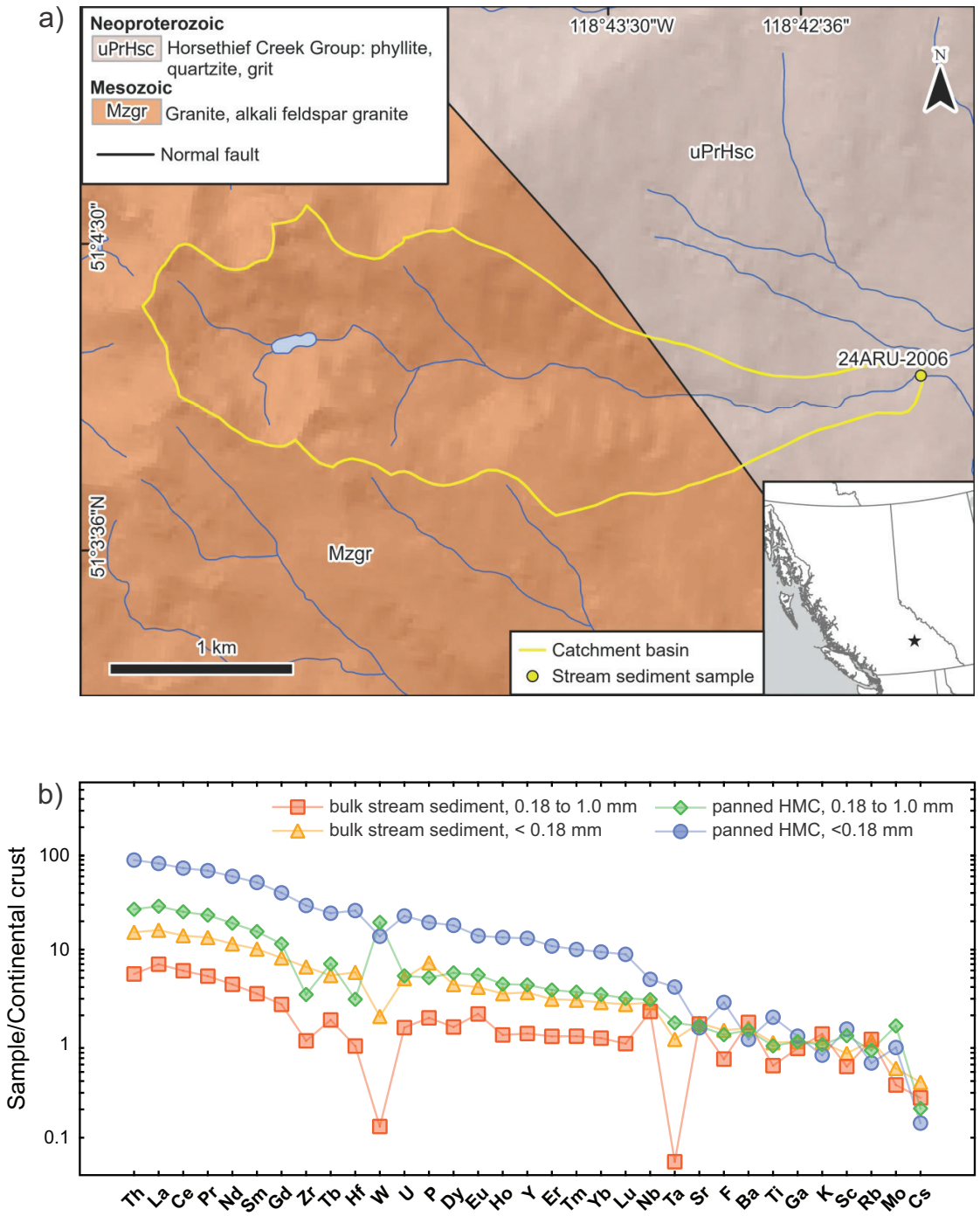

Fig. 13. a) Sampling site and catchment basin (area=3.66 km^2) at the Regional Geochemical Survey (RGS) rare-metal anomaly 27 (Rukhlov et al., 2024), Perry River valley (82M/02). Geology after Wheeler and Fox (1964), Höy and Brown (1980), Johnson (1990), Logan (2002), and Cui et al. (2017). **b)** Bulk stream-sediment and panned, heavy mineral concentrate (HMC) data normalized to bulk continental crust values of Rudnick and Gao (2014).

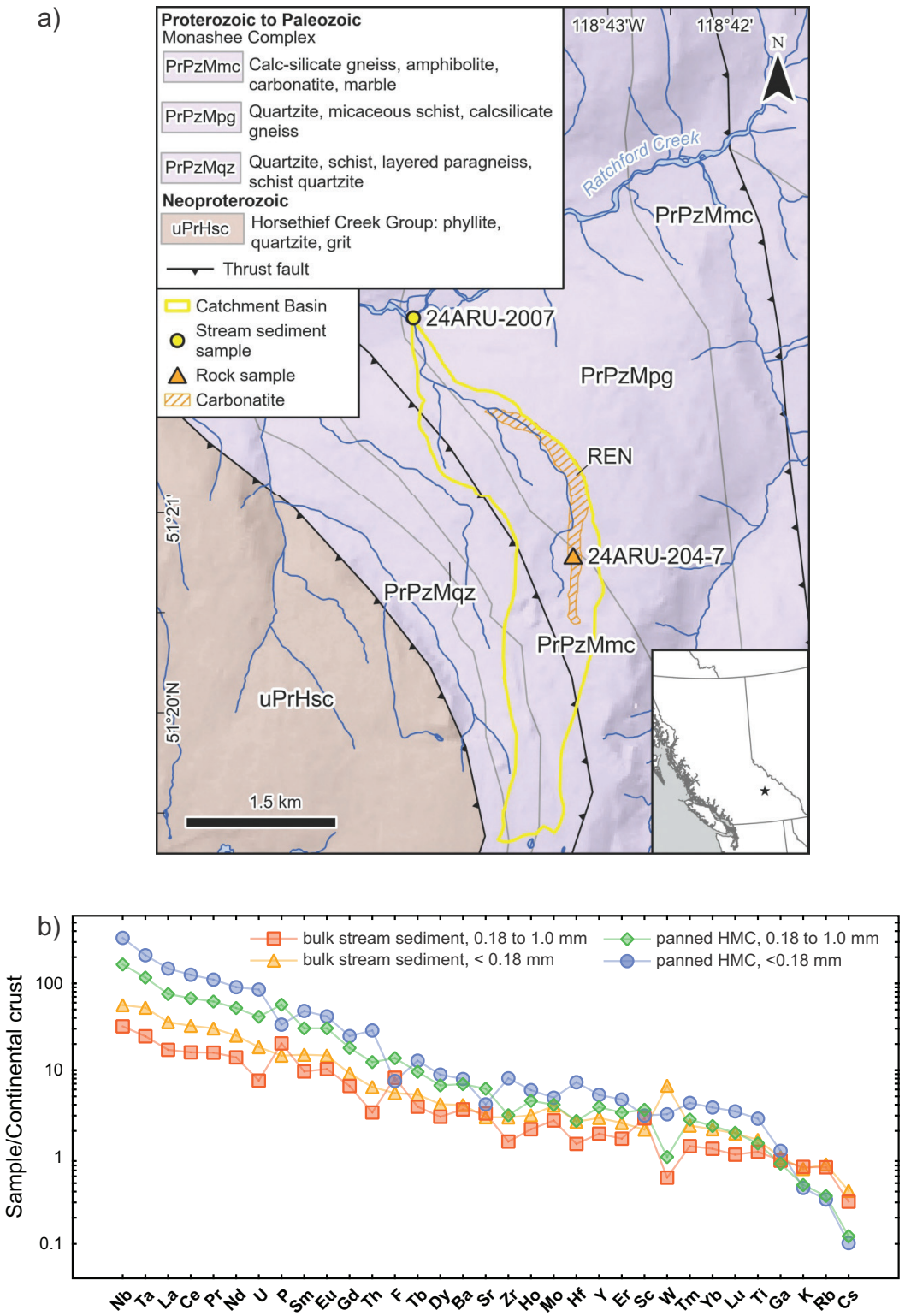

Fig. 14. a) Sampling sites and catchment basin (area=3.85 km^2) downstream of Ren (Ratchford Creek) carbonatite, Ratchford Creek valley (82M/07). Carbonatite footprint after Ya'acoby (2014). Geology after Wheeler and Fox (1964), Höy and Brown (1980), Logan (2002), and Cui et al. (2017). **b)** Bulk stream-sediment and panned, heavy mineral concentrate (HMC) data normalized to bulk continental crust values of Rudnick and Gao (2014).

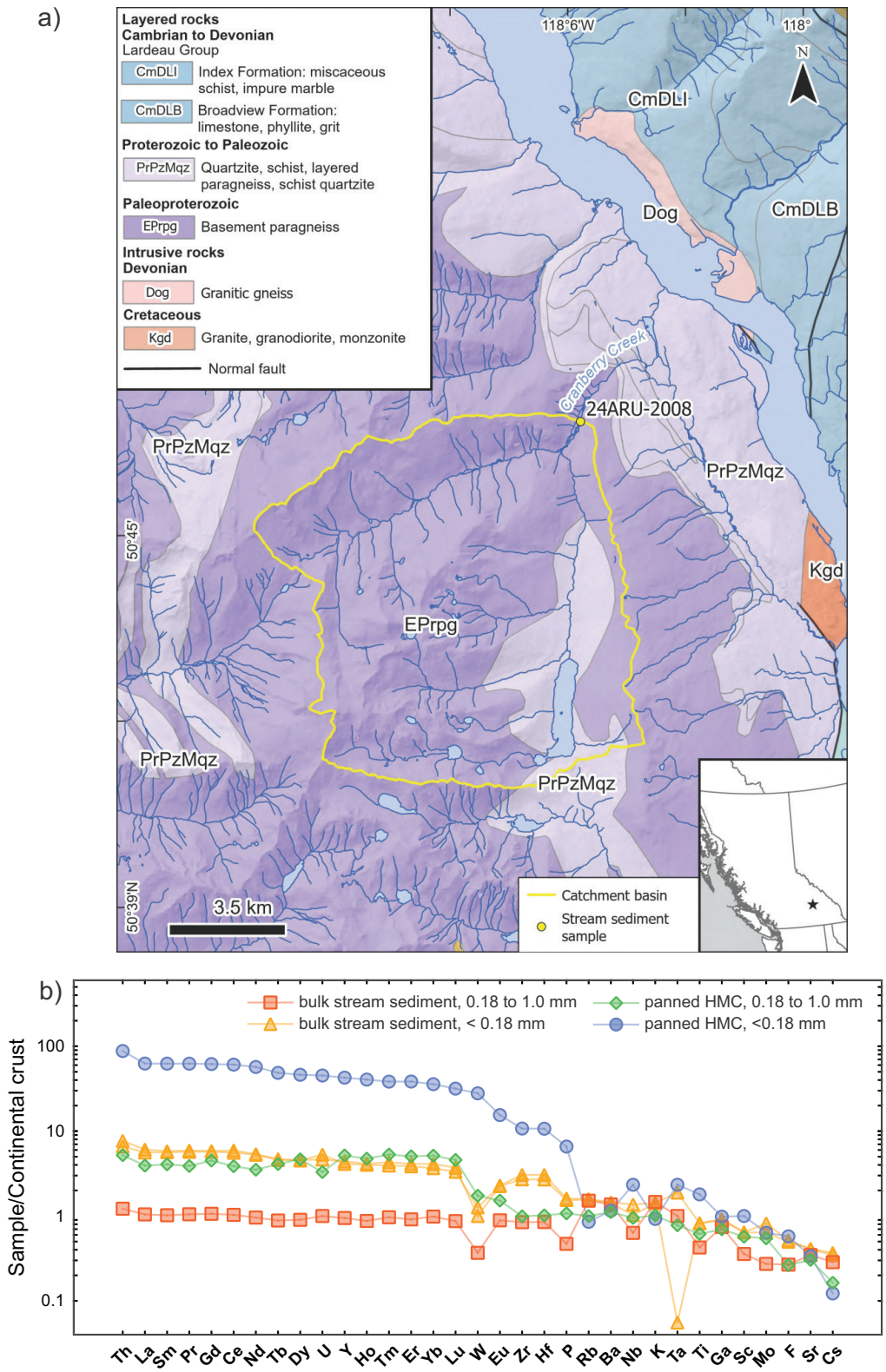

Fig. 15. a) Sampling site and catchment basin (area=96.51 km^2) at Cranberry Creek, downstream of the Regional Geochemical Survey (RGS) rare-metal anomalies 20 and 21 (82M/07; Rukhlov et al., 2024). Geology after Rice and Jones (1960), Logan (2002), Thompson et al. (2006), Cui et al. (2017). **b)** Bulk stream-sediment and panned, heavy mineral concentrate (HMC) data normalized to bulk continental crust values of Rudnick and Gao (2014).

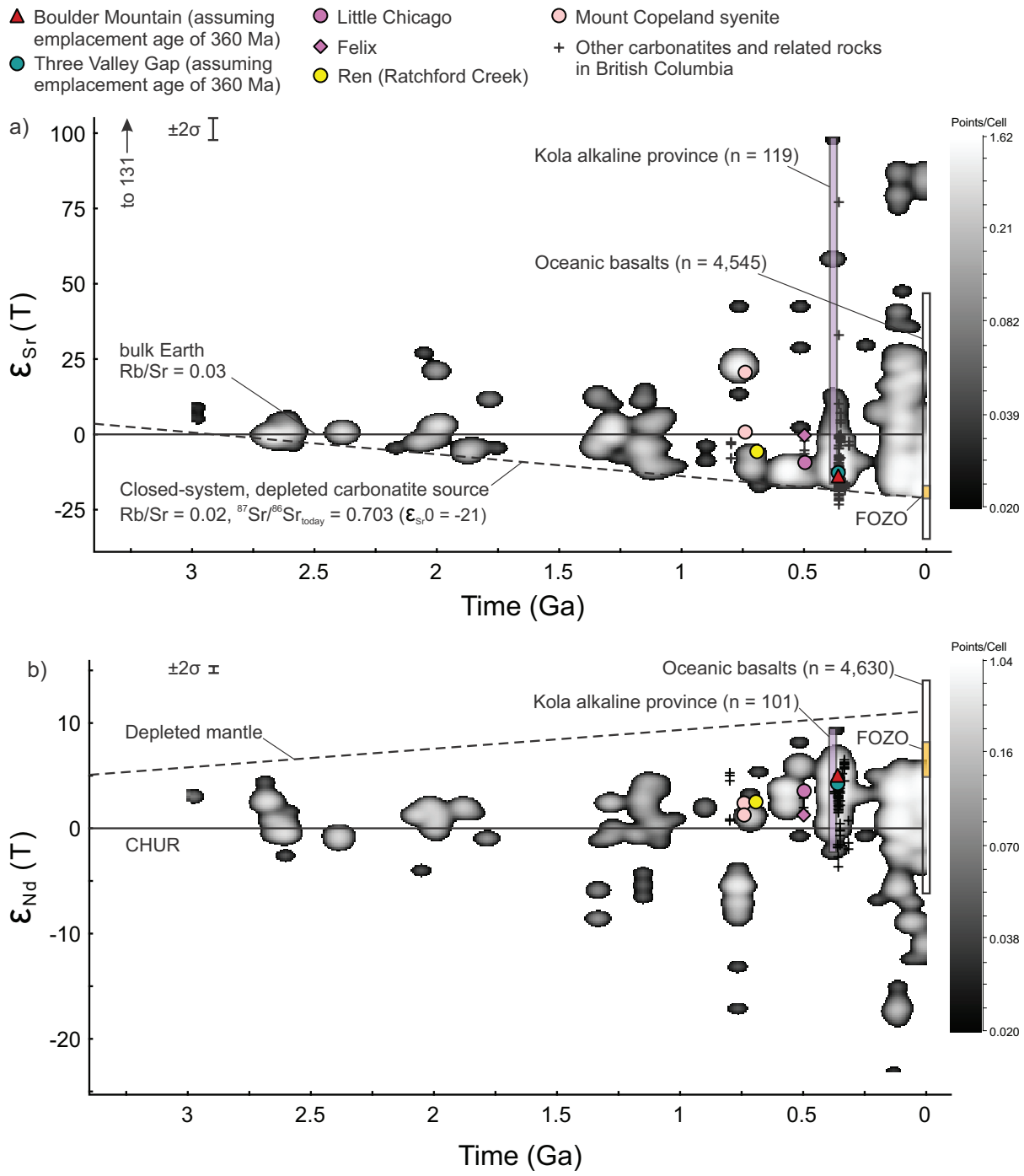

Fig. 16. Sr and Nd evolution diagrams for carbonatites and related rocks in British Columbia (including data in Han et al., 2025); the range of initial $^{87}Sr/^{86}Sr$ and initial $^{143}Nd/^{144}Nd$ values from ca. 0.37 Ga Kola alkaline province (shaded rectangle) after Rukhlov et al. (2015); the range of present-day $^{87}Sr/^{86}Sr$ and $^{143}Nd/^{144}Nd$ values in mid-ocean ridge and ocean island basalts (open rectangle) after Stracke (2012); grayscale heat maps corresponding to the density of the global carbonatite data (n = 589/500) after Rukhlov et al. (2015); 'FOcus ZOne' (FOZO) mantle component after Hart et al. (1992), Stracke et al. (2005), and Stracke (2012). **a)** Time (billions of years) versus $\varepsilon_{Sr}(T)$; $\varepsilon_{Sr}(T) = [(^{87}Sr/^{86}Sr_{sample}/ {}^{87}Sr/^{86}Sr_{bulk\ Earth}) - 1]\cdot 10^4$, where $^{87}Sr/^{86}Sr_{sample}$ is the initial ratio in the sample and $^{87}Sr/^{86}Sr_{bulk\ Earth}$ is the ratio in the bulk Earth (solid line; after DePaolo and Wasserburg, 1976; DePaolo, 1988) at that time; closed-system, depleted carbonatite source (dashed line) after Rukhlov et al. (2015); $\varepsilon_{Sr}(T)$ value of 131 in whole rock eudialyte syenite from Ice River (Locock, 1994). **b)** Time (billions of years) versus $\varepsilon_{Nd}(T) = (^{143}Nd/^{144}Nd_{sample}/^{143}Nd/^{144}Nd_{CHUR}) - 1]\cdot 10^4$, where $^{143}Nd/^{144}Nd_{sample}$ is the initial ratio in the sample and $^{143}Nd/^{144}Nd_{CHUR}$ is the ratio in the chondritic uniform reservoir (CHUR, solid line; after Jacobsen and Wasserburg, 1980; Hamilton et al., 1983) at that time; depleted mantle model (dashed line) after Rehkämper and Hofmann (1997).

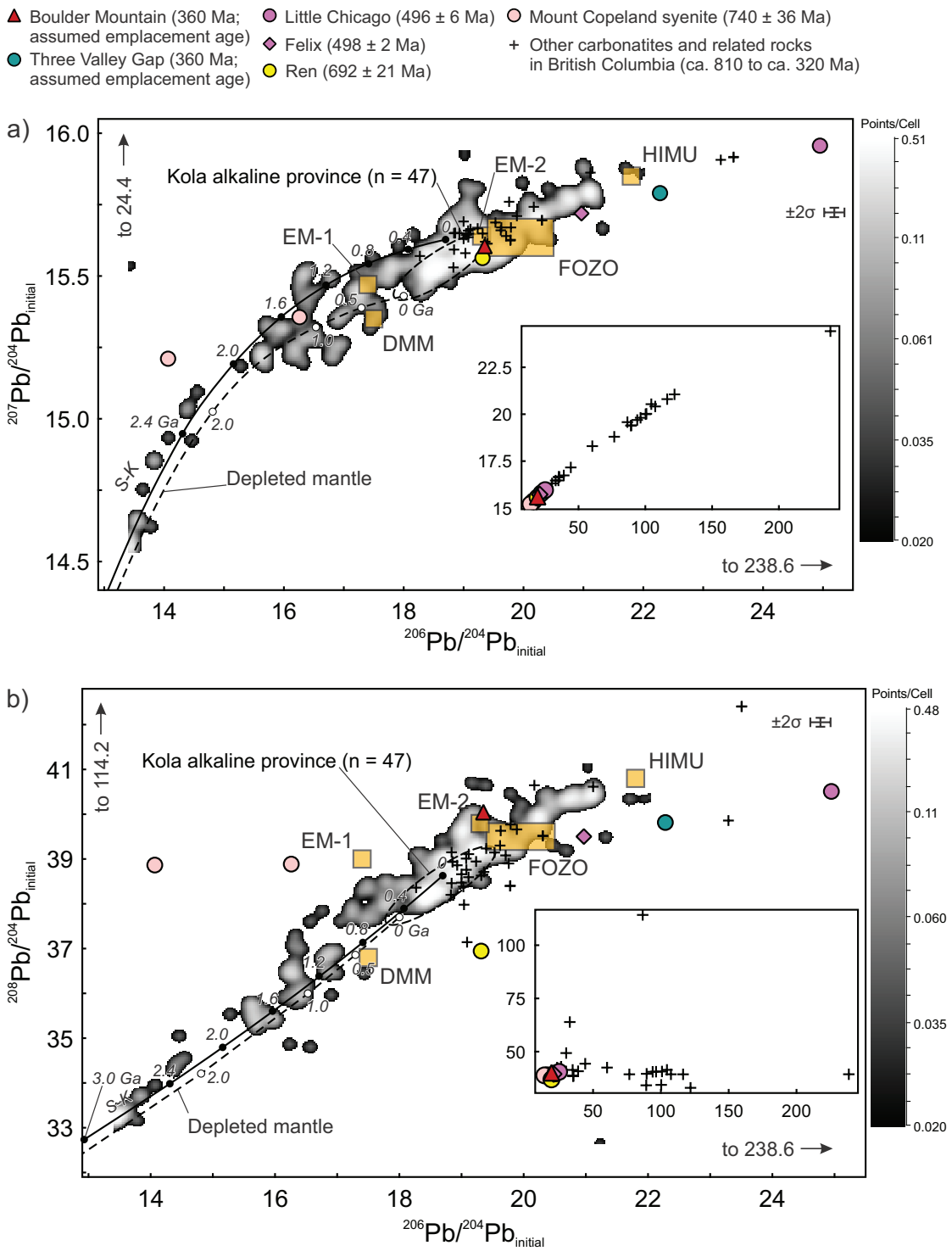

Fig. 17. Pb-Pb isotope correlation diagrams for ca. 0.80 to 0.32 Ga carbonatites and related alkaline rocks in British Columbia (including data in Han et al., 2025); grayscale heat maps corresponding to the density of the data from ca. 3 to 0 Ga carbonatites worldwide (n = 282), including the ca. 0.37 Ga Kola alkaline province after Rukhlov et al. (2015); Mahalanobis distance at $\chi 2 = 0.99$ (ellipse) using robust multivariate estimation (Cambell, 1980). **a)** Initial $^{206}Pb/^{204}Pb$ versus initial $^{207}Pb/^{204}Pb$. **b)** Initial $^{206}Pb/^{204}Pb$ versus initial $^{208}Pb/^{204}Pb$. Second-stage growth curve (*S-K*) for terrestrial lead isotopic evolution (solid line) after Stacey and Kramers (1975). Depleted mantle evolution (dashed line) assuming initial Earth $^{206}Pb/^{204}Pb$, $^{207}Pb/^{204}Pb$, and $^{208}Pb/^{204}Pb$ ratios taken from Canyon Diablo troilite values (Tatsumoto et al., 1973), $^{238}U/^{204}Pb = 0.7$ at 4.57 Ga (after Allègre et al., 1995) and closed-system evolution from 4.43 Ga (Doe and Stacey, 1974; Wood et al., 2008; Maltese and Mezger, 2020) to present-day values of Rehkämper and Hofmann (1997). Present-day depleted, mid-ocean ridge mantle (DMM), enriched mantle 1 and 2 (EM-1 and EM-2), 'FOcus ZOne' (FOZO), and high-$^{238}U/^{204}Pb$ or μ (HIMU) mantle components after Hart et al. (1992), Stracke et al. (2005), and Stracke (2012). Extremely radiogenic initial $^{206}Pb/^{204}Pb$ (up to 238.6), $^{207}Pb/^{204}Pb$ (up to 24.4), and $^{208}Pb/^{204}Pb$ (up to 114.2) in apatite, carbonate, and molybdenite fractions from British Columbia carbonatites (Rukhlov et al., 2018; Han et al., 2025).

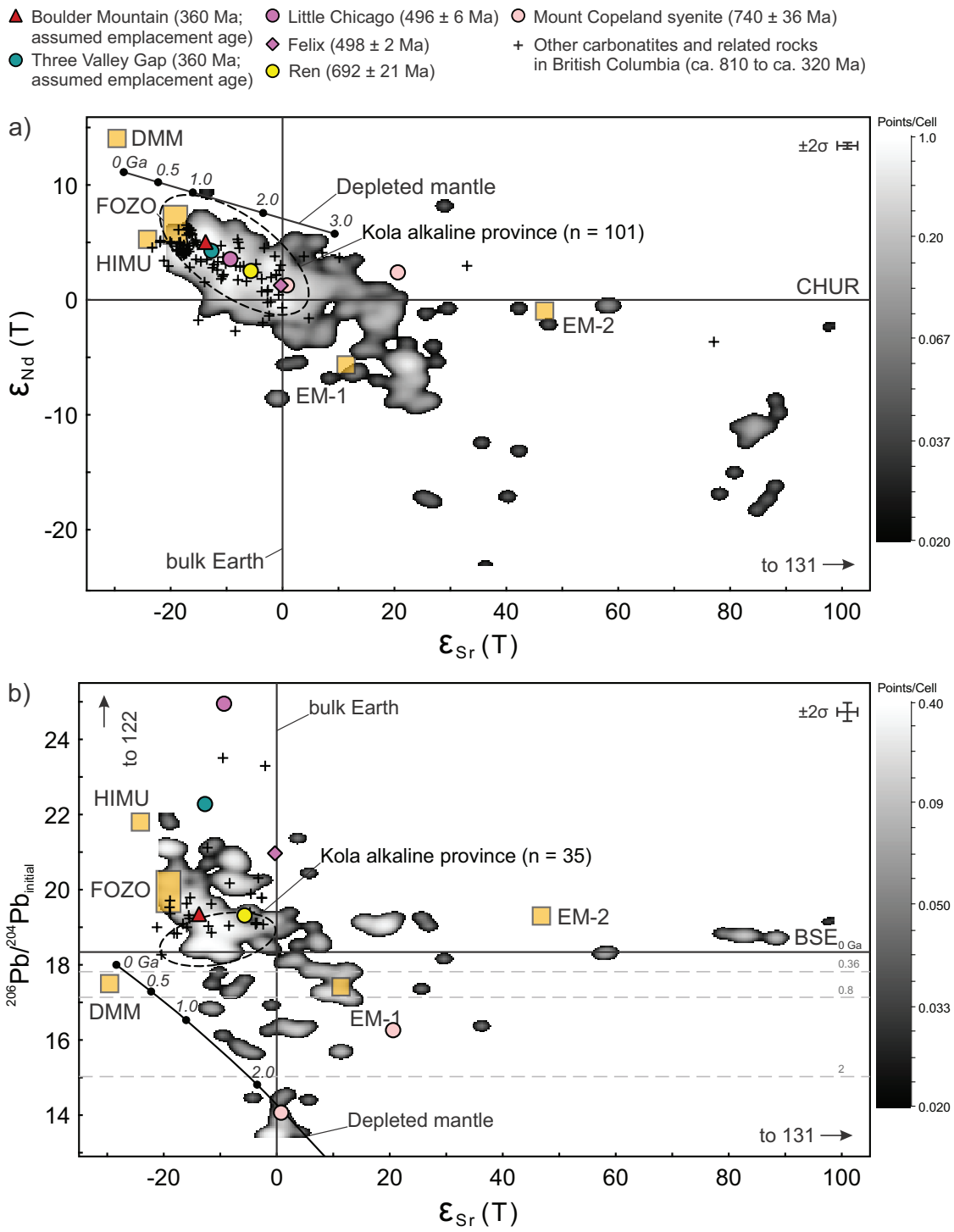

Fig. 18. Sr-Pb-Nd isotope correlation diagrams for ca. 0.80 to 0.32 Ga carbonatites and related alkaline rocks in British Columbia (including data in Han et al., 2025); grayscale heat maps corresponding to the density of the data from ca. 3 to 0 Ga carbonatites worldwide (n = 490/224), including the ca. 0.37 Ga Kola alkaline province after Rukhlov et al. (2015); Mahalanobis distance at $\chi 2 = 0.99$ (ellipse) using robust multivariate estimation (Cambell, 1980). **a)** $\varepsilon_{Sr}(T)$ versus $\varepsilon_{Nd}(T)$; $\varepsilon_{Sr}(T) = [(^{87}Sr/^{86}Sr_{sample}/^{87}Sr/^{86}Sr_{bulk\ Earth}) - 1]\cdot 10^4$, where $^{87}Sr/^{86}Sr_{sample}$ is the initial ratio in the sample and $^{87}Sr/^{86}Sr_{bulk\ Earth}$ is the ratio in the bulk Earth (after DePaolo and Wasserburg, 1976; DePaolo, 1988) at that time; $\varepsilon_{Sr}(T)$ value of 131 in whole rock eudialyte syenite from Ice River (Locock, 1994); $\varepsilon_{Nd}(T) = [(^{143}Nd/^{144}Nd_{sample}/^{143}Nd/^{144}Nd_{CHUR}) - 1]\cdot 10^4$, where $^{143}Nd/^{144}Nd_{sample}$ is the initial ratio in the sample and $^{143}Nd/^{144}Nd_{CHUR}$ is the ratio in the chondritic uniform reservoir (CHUR; after Jacobsen and Wasserburg, 1980; Hamilton et al., 1983) at that time. **b)** $\varepsilon_{Sr}(T)$ versus initial $^{206}Pb/^{204}Pb$; bulk silicate Earth (BSE) parameters after Allègre and Lewin (1989); extremely radiogenic initial $^{206}Pb/^{204}Pb$ values up to 122 in apatite and carbonate fractions from British Columbia carbonatites (Han et al., 2025). Present-day depleted, mid-ocean ridge mantle (DMM), enriched mantle 1 and 2 (EM-1 and EM-2), 'FOcus ZOne' (FOZO), and high-$^{238}U/^{204}Pb$ or μ (HIMU) mantle components after Hart et al. (1992), Stracke et al. (2005), and Stracke (2012). Depleted mantle evolution model curve after Rehkämper and Hofmann (1997).

In the Sr-Pb-Nd isotopic correlation diagrams (Fig. 18) excluding the extremely high initial $^{206}Pb/^{204}Pb$ values as discussed above, the British Columbia carbonatites and related rocks partly overlap the data from ca. 0.37 Ga Kola alkaline province (Rukhlov et al., 2015) and the oceanic signatures (Hart et al., 1992; Stracke et al., 2005; Stracke, 2012). The depleted mid-ocean ridge mantle end-member (Fig. 18) represents shallow asthenospheric mantle, but it appears to have played little, if any, role in the mantle source of carbonatites, including the British Columbia examples. Rather, the Sr-Pb-Nd data suggest a heterogeneous mantle source with mixing arrays involving the 'FOcus ZOne' (FOZO) mantle end-member (Figs. 16-18) found in hot spots and the plume-related Kola alkaline province (ca. 0.37 Ga; for an overview, see Bell and Rukhlov, 2004; Rukhlov et al., 2015 and references therein) and considered to be relatively primitive and of deep mantle origin (Hart et al., 1992; Hauri et al., 1994; Bell and Tilton, 2002; Campbell and O'Neill, 2012). Thus, despite protracted deformation and upper amphibolite-facies metamorphism, the British Columbia examples are isotopically indistinguishable from worldwide carbonatites generated by deep-mantle plumes (Rukhlov et al., 2018, 2019).

7. Conclusions

Stream-sediment lithochemical orientation downstream of known carbonatites and related rocks reveals multi-element dispersion haloes of REE, Nb, Ta and other indicator elements. Panned heavy mineral concentrates (HMC) show up to 100 times background (average continental crust) contrast and is thus the preferred sample medium for REE and rare-metal prospecting. The new Re-Os model age of 55.94 ±0.23 (2σ) Ma on molybdenite from past-producing Mount Copeland molybdenum mine links mineralization to Paleogene metamorphic overprint of a body that initially crystallized at ca. 740 Ma. The Sr-Pb-Nd isotopic data from ca. 800-690 Ma, 500 Ma, and ca. 370-320 Ma carbonatites and related rocks in British Columbia follow the trend defined by carbonatites worldwide. These rocks record the evolution of a primitive mantle source that has behaved as a relatively closed-system, at least during the last 3 Ga of Earth history, with the present-day, isotopic attributes similar to FOZO that may represent the relatively primitive, deep mantle.

Acknowledgments

We thank K. McLaren (BC Geological Survey) for geospatial support and digital data capture, S. Barker (Mineral Deposits Research Unit, University of British Columbia) for help with acquiring Axioscan imagery, Glacier Helicopters Ltd. and Yellowhead Helicopters Ltd. for logistical support in the field, and ALS Canada Ltd. and Bureau Veritas Commodities Canada Ltd. for assays. F. Horton (Woods Hole Oceanographic Institution) and M.F. Hardman (Gemological Institute of America) provided thorough reviews and many helpful comments.

References cited

Allègre, C.J., and Lewin, E., 1989. Chemical structure and history of the Earth, evidence from global non-linear inversion of isotopic data in a three-box model. Earth and Planetary Science Letters, 96, 61-88.

Allègre, C.J., Manhes, G., and Gopel, C., 1995. The age of the Earth. Geochimica et Cosmochimica Acta, 59, 1445-1456.

Andersen, T., and Taylor, P.N., 1988. Pb isotope geochemistry of the Fen carbonatite complex, S.E. Norway: Age and petrogenetic implications. Geochimica et Cosmochimica Acta, 52, 209-215.

Bell, K., (Ed.), 1989. Carbonatites: Genesis and Evolution. Unwin Hyman, London, United Kingdom, 618 p.

Bell, K., and Rukhlov, A.S., 2004. Carbonatites from the Kola Alkaline Province: origin, evolution and source characteristics. In: Phoscorites and Carbonatites from Mantle to Mine: The Key Example of the Kola Alkaline Province, Wall, F., and Zaitsev, A.N., (Eds.), Mineralogical Society Series, 10, The Mineralogical Society, London, United Kingdom, pp. 433-468.

Bell, K., and Tilton, G.R., 2002. Probing the mantle: the story from carbonatites. American Geophysical Union, Eos Transactions, 83, 273, 276-277.

Bell, K., Kjarsgaard, B.A., and Simonetti, A., (Eds.), 1998. Carbonatites-into the twenty-first century. Journal of Petrology, 39 (11-12), 1839-2154.

Belousova, E.A., Griffin, W.L., O'Reilly. S.Y., and Fisher, N.I., 2002. Igneous zircon: trace element composition as an indicator of source rock type. Contributions to Mineralogy and Petrology, 143, 602-622.

Brown, J.A., 2012. 2011 geological, geochemical, geophysical, and mineralogical assessment report at the Kin-Trident REE-Nb-Mo project. British Columbia Ministry of Energy, Mines and Natural Gas, British Columbia Geological Survey, Assessment Report 32655, 40 p.

Campbell, R.B., 1968. Geology, Canoe River, British Columbia. Geological Survey of Canada, Preliminary Map 15-1967, 1:253,400 scale.

Campbell, N.A., 1980. Robust procedures in multivariate analysis. I: Robust covariance estimation. Journal of the Royal Statistical Society, Series C: Applied Statistics, 29, 231-237.

Campbell, I.H., and O'Neill, H.St.C., 2012. Evidence against a chondritic Earth. Nature, 483, 553-558.

Chakhmouradian, A.R., Reguir, E.P., Kressall, R.D., Crozier, J., Pisiak, L.K., Sidhu, R., and Yang, P., 2015. Carbonatite-hosted niobium deposit at Aley, northern British Columbia (Canada): Mineralogy, geochemistry and petrogenesis. Ore Geology Reviews, 64, 642-666.

Chen, W., Lu, J., Jiang, S.Y., Ying, Y.C., and Liu, Y.S., 2018. Radiogenic Pb reservoir contributes to the rare earth element (REE) enrichment in South Qinling carbonatites. Chemical Geology, 494, 80-95.

Chudy, T.C., 2013. The petrogenesis of the Ta-bearing Fir carbonatite system, east-central British Columbia, Canada. Unpublished Ph.D. thesis, University of British Columbia, Canada, 316 p.

Çimen, O., Kuebler, C., Monaco, B., Simonetti, S.S., Corcoran, L., Chen, W., and Simonetti, A., 2018. Boron, carbon, oxygen and radiogenic isotope investigation of carbonatite from the Miaoya complex, central China: Evidences for late-stage REE hydrothermal event and mantle source heterogeneity. Lithos, 322, 225-237.

Çimen, O., Kuebler, C., Simonetti, S.S., Corcoran, L., Mitchell, R.H., and Simonetti, A., 2019. Combined boron, radiogenic (Nd, Pb, Sr), stable (C, O) isotopic and geochemical investigations of carbonatites from the Blue River Region, British Columbia (Canada): Implications for mantle sources and recycling of crustal carbon. Chemical Geology, 529, 119240. <https://doi.org/10.1016/j.chemgeo.2019.07.015>

Colpron, M., 2020. Yukon terranes-A digital atlas of terranes for the northern Cordillera. Yukon Geological Survey. <https://data.geology.gov.yk.ca/Compilation/2#InfoTab>

Crowley, J.L., and Parrish, R.R., 1999. U-Pb isotopic constraints on diachronous metamorphism in the northern Monashee complex, southern Canadian Cordillera. Journal of Metamorphic Geology, 17, 483-502.

Cui, Y., Miller, D., Schiarizza, P., and Diakow, L.J., (compilers), 2017. British Columbia digital geology. British Columbia Ministry of Energy, Mines and Petroleum Resources, British Columbia Geological Survey Open File 2017-8, 9p. Data version 2021-12-19.

Currie, K.L., 1976. The alkaline rocks of Canada. Geological Survey of Canada, Bulletin 239, 228 p.

Dalsin, M.L., Groat, L.A., Creighton, S., and Evans, R.J., 2015. The mineralogy and geochemistry of the Wicheeda carbonatite complex, British Columbia, Canada. Ore Geology Reviews, 64, 523-542.

DePaolo, D.J., 1988. Neodymium Isotopes in Geology. Springer-Verlag, 187 p.

DePaolo, D.J., and Wasserburg, G.J., 1976. Inferences about magma sources and mantle structure from variations of $^{143}Nd/^{144}Nd$. Geophysical Research Letters, 3, 743-746.

DIGIS Team, 2023. GEOROC compilation: Ocean Island groups. GRO data, V9, Göttingen University, Göttingen, Germany. <https://doi.org/10.25625/WFJZKY>

Doe, B.R., and Stacey, J.S., 1974. The application of lead isotopes to the problems of ore genesis and ore prospect evaluation: a review. Economic Geology, 69, 757-776.

Gammons, C.H., Risedorf, S., Wyss, G., and Lowers, H., 2024. Occurrences of the rare, REE minerals daqingshanite, törnebohmite, biraite, sahamalite, and ferriperbøeite from the Sheep Creek area, Montana, USA. Minerals 2024, 14, 1047. <https://doi.org/10.3390/min14101047>

Hamilton, P.J., O'Nions, R.K., Bridgwater, D., and Nutman, A., 1983. Sm-Nd studies of Archaean metasediments and metavolcanics from West Greenland and their implications for the Earth's early history. Earth and Planetary Science Letters, 62, 263-272.

Han, T., Ootes, L., Rukhlov, A.S., and Angelo, T., 2025. Radiogenic isotope compilation. British Columbia Ministry of Mining and Critical Minerals, British Columbia Geological Survey GeoFile 2025-08, in press.

Hart, S.R., Hauri, E.H., Oschmann, L.A., and Whitehead, J.A., 1992. Mantle plumes and entrainment: isotopic evidence. Science, 256, 517-520.

Hauri, E.H., Whitehead, J.A., and Hart, S.R., 1994. Fluid dynamic and geochemical aspects of entrainment in mantle plumes. Journal of Geophysical Research, 99(B12), 24275-24300.

Hickin, A.S., Ootes, L., Brzozowski, M.J., Northcote, B., Rukhlov, A.S., Bain, W.M., and Orovan, E.A., 2024. Critical minerals and mineral systems in British Columbia. In: Geological Fieldwork 2023, British Columbia Ministry of Energy, Mines and Low Carbon Innovation, British Columbia Geological Survey Paper 2024-01, pp. 13-51.

Höy, T., 1988. Geology of the Cottonbelt lead-zinc-magnetite layer, carbonatites and alkaline rocks in the Mount Grace area, Frenchman Cap dome, southeastern British Columbia. British Columbia Ministry of Energy, Mines and Petroleum Resources, British Columbia Geological Survey Bulletin 80, 99 p., 1:25,000-scale map.

Höy, T., and Brown, R.L., 1980. Geology of the eastern margin of Shuswap Complex, Frenchman Cap area. British Columbia Ministry of Energy, Mines and Petroleum Resources, British Columbia Geological Survey Preliminary Map 43, 1:100,000 scale.

Jacobsen, S.B., and Wasserburg, G.J., 1980. Sm-Nd isotopic evolution of chondrites. Earth and Planetary Science Letters, 50, 139-155.

Johnson, B.J., 1990. Geology adjacent to the western margin of the Shuswap metamorphic complex (parts of NTS 82L, M). British Columbia Ministry of Energy, Mines and Petroleum Resources, British Columbia Geological Survey Open File 1990-30, 1:100,000 scale.

Kelemen, P.B., Hanghøj, K., and Greene, A.R., 2014. One view of the geochemistry of subduction-related magmatic arcs, with an emphasis on primitive andesite and lower crust. In: The Crust, Treatise on Geochemistry, 2nd Edition, Volume 4, Holland, H.D., Turekian, K.K., and Rudnick, R.L., (Eds.), Elsievier, Amsterdam, pp. 749-806. <https://doi.org/10.1016/B978-0-08-095975-7.00323-5>

Kulla, G., and Hardy, J., 2015. Commerce Resources Corp. Blue River tantalum-niobium project, British Columbia, Canada, project update report. NI 43-101 Technical Report, 138 p.

Lett, R., and Rukhlov, A.S., 2017. A review of analytical methods for regional geochemical survey (RGS) programs in the Canadian Cordillera. In: Indicator Minerals in Till and Stream Sediments of the Canadian Cordillera, Ferbey, T., Plouffe, A., and Hickin, A.S., (Eds.), Geological Association of Canada Special Paper Volume 50, and Mineralogical Association of Canada Topics in Mineral Sciences Volume 47, pp. 53-108.

Locock, A.J., 1994. Aspects of the geochemistry and mineralogy of the Ice River alkaline intrusive complex, Yoho National Park, British Columbia. Unpublished M.Sc. thesis, University of Alberta, Canada, 163 p.

Logan, J.M., (compiler), 2002. Intrusion-related mineral occurrences of the Cretaceous Bayonne magmatic belt, southeast British Columbia. British Columbia Ministry of Energy and Mines, British Columbia Geological Survey Geoscience Map 2002-01, 1:500,000 scale.

Mackay, D.A.R., and Simandl, G.J., 2015. Pyrochlore and columbite-tantalite as indicator minerals for specialty metal deposits. Geochemistry: Exploration, Environment, Analysis, 15, 167-178.

Mäder, U.K., 1987. The Aley carbonatite complex, northern Rocky Mountains, British Columbia (94B/5). In: Geological Fieldwork 1986, British Columbia Ministry of Energy, Mines and Petroleum Resources, British Columbia Geological Survey Paper 1987-1, pp. 283-288.

Maltese, A., and Mezger, K., 2020. The Pb isotope evolution of Bulk Silicate Earth: Constraints from its accretion and early differentiation history. Geochimica et Cosmochimica Acta, 271, 179-193.

Mao, M., Rukhlov, A.S., Rowins, S.M., Spence, J., and Coogan, L.A., 2016. Apatite trace element compositions: A robust new tool for mineral exploration. Economic Geology, 111, 1187-1222.

McDonough, M.R., Simony, P.S., Morrison, M.L., Oke, C., Sevigny, J.H., Robbins, D.B., Seigel, S.G., and Grasby, S.E., 1991. Howard Creek, British Columbia. Geological Survey of Canada, Open File 2411, 1:50,000 scale.

McDonough, M.R., Simony, P.S., Sevigny, J.H., Robbins, D.B., Raeside, R., Doucet, P., Pell, J., and Dechesne, R.G., 1992. Geology of Nagle Creek and Blue River, British Columbia (83D/2 and 83D/3). Geological Survey of Canada, Open File 2512, 1:50,000 scale.

Millonig, L.J., and Groat, L.A., 2013. Carbonatites in western North America-occurrences and metallogeny. In: Tectonics, Metallogeny, and Discovery: The North American Cordillera and Similar Accretionary Settings, Colpron, M., Bissig, T., Rusk, B.G., and Thompson, F.H. (Eds.), Society of Economic Geologists, Special Publication 17, pp. 245-264.

Millonig, L.J., Gerdes, A., and Groat, L.A., 2012. U-Th-Pb geochronology of meta-carbonatites and meta-alkaline rocks in the southern Canadian Cordillera: a geodynamic perspective. Lithos, 152, 202-217.

Millonig, L.J., Gerdes, A., and Groat, L.A., 2013. The effect of amphibolite facies metamorphism on the U-Th-Pb geochronology of accessory minerals from meta-carbonatites and associated meta-alkaline rocks. Chemical Geology, 353, 199-209.

Murphy, D.C., (compiler), 2007. Geology, Canoe River, British Columbia-Alberta. Geological Survey of Canada, Map 2110A, 1:250,000 scale.

Nelson, J.L., Colpron, M., and Israel, S., 2013. The Cordillera of British Columbia, Yukon and Alaska: tectonics and metallogeny. In: Tectonics, Metallogeny, and Discovery: The North American Cordillera and Similar Accretionary Settings, Colpron, M., Bissig, T., Rusk, B.G., and Thompson, F.H., (Eds.), Society of Economic Geologists, Special Publication 17, pp. 53-109.

Okulitch, A.V., Loveridge, W.D., and Sullivan, R.W., 1981. Preliminary radiometric analyses of zircons from the Mount Copeland syenite gneiss, Shuswap metamorphic complex, British Columbia. In: Current Research, Part A, Geological Survey of Canada, Paper 81-1A, pp. 33-36.

Parrish, R.R., 1995. Thermal evolution of the southeastern Canadian Cordillera. Canadian Journal of Earth Sciences, 32, 1618-1642.

Parrish, R.R., and Scammell, R.J., 1988. The age of the Mount Copeland syenite gneiss and its metamorphic zircons, Monashee complex, southeastern British Columbia. In: Radiogenic Age and Isotopic Studies: Report 2, Geological Survey of Canada, Paper 88-2, pp. 21-28.

Pell, J., 1994. Carbonatites, nepheline syenites, kimberlites and related rocks in B.C. British Columbia Ministry of Energy, Mines and Petroleum Resources, British Columbia Geological Survey, Bulletin 88, 136 p.

Pell, J., and Simony, P.S., 1987. New correlations of Hadrynian strata, south-central British Columbia. Canadian Journal of Earth Sciences, 24, 302-313.

Raeside, R.P., and Simony, P.S., 1983. Stratigraphy and deformational history of the Scrip Nappe, Monashee Mountains, British Columbia. Canadian Journal of Earth Sciences, 20, 639-650.

Rehkämper, M., and Hofmann, A.W., 1997. Recycled ocean crust and sediment in Indian Ocean MORB. Earth and Planetary Science Letters, 147, 93-106. <https://doi.org/10.1016/S0012-821X(97)00009-5>

Rice, H.M.A., and Jones, A.G., 1960. Geology, Vernon, Kamloops, Osoyoos, and Kootenay districts, British Columbia. Geological Survey of Canada, "A" Series Map, 1059A, 1:253,440 scale.

Rudnick, R.L., and Gao, S., 2014. Composition of the continental crust. In: The Crust, Treatise on Geochemistry, 2nd Edition, Volume 4, Holland, H.D., Turekian, K.K., and Rudnick, R.L., (Eds.), Elsievier, Amsterdam, pp. 1-51. <http://dx.doi.org/10.1016/B978-0-08-095975-7.00301-6>

Rukhlov, A.S., and Bell, K., 2010. Geochronology of carbonatites from the Canadian and Baltic Shields, and the Canadian Cordillera: clues to mantle evolution. Mineralogy and Petrology, 98, 11-54.

Rukhlov, A.S., Bell, K., and Amelin, Y., 2015. Carbonatites, isotopes and evolution of the subcontinental mantle: An overview. In: Symposium on Strategic and Critical Materials Proceedings, November 13-14, 2015, Victoria, British Columbia, Simandl, G.J. and Neetz, M., (Eds.), British Columbia Ministry of Energy and Mines, British Columbia Geological Survey Paper 2015-3, pp. 39-64.

Rukhlov, A.S., Chudy, T.C., Arnold, H., and Miller, D., 2018. Field trip guidebook to the Upper Fir carbonatite-hosted Ta-Nb deposit, Blue River area, east-central British Columbia. British Columbia Ministry of Energy, Mines and Petroleum Resources, British Columbia Geological Survey, GeoFile 2018-6, 67 p.

Rukhlov, A.S., Aspler, L.B., and Gabites, J., 2019. Are Cordilleran carbonatite hosts of Ta, Nb and REE from the deep mantle? British Columbia Ministry of Energy, Mines and Petroleum Resources, British Columbia Geological Survey GeoFile 2019-08.

Rukhlov, A.S., Coats, B., Van der Vlugt, J., Beaupre-Olsen, I.J., and Zaborniak, K., 2023. British Columbia Geological Survey sample archive: An emerging resource for public geoscience. In: Geological Fieldwork 2022, British Columbia Ministry of Energy, Mines and Low Carbon Innovation, British Columbia Geological Survey Paper 2023-1, pp. 85-90.

Rukhlov, A.S., Cui, Y., Cunningham, Q., Fortin, G., and Anderson, C., 2024. Geochemical signals of carbonatite-related critical metals in provincial stream sediments. In: Geological Fieldwork 2023, British Columbia Ministry of Energy, Mines and Low Carbon Innovation, British Columbia Geological Survey Paper 2024-01, pp. 97-122.

Rukhlov, A.S., Ootes, L., Creaser, R.A., Cunningham, Q.F., de Waal, F.S., and Wenger, D.K., 2025. Supplementary data for British Columbia carbonatites revisited: New whole rock Sr-Pb-Nd isotopic insights and drainage prospectivity trends. British Columbia Ministry of Mining and Critical Minerals, British Columbia Geological Survey GeoFile 2025-09, in press.

Scammell, R.J., 1987. Stratigraphy, structure and metamorphism of the north flank of the Monashee complex, southeastern British Columbia: a record of Proterozoic extension and Phanerozoic crustal thickening. Unpublished M.Sc. thesis, Carleton University, Ottawa, Canada, 205 p.

Scammell, R.J., 1993. Mid-Cretaceous to Tertiary thermotectonic history of former mid-crustal rocks, southern Omineca belt, Canadian Cordillera. Unpublished Ph.D. thesis, Queens University, Kingston, Ontario, 576 p.

Scammell, R.J., and Brown, R.L., 1990. Cover gneisses of the Monashee terrane: a record of syn-sedimentary rifting in the North American Cordillera. Canadian Journal of Earth Sciences, 27, 712-726.

Schmidt, M.W., Giuliani, A., and Poli, S., 2024. The origin of carbonatites-combining the rock record with available experimental constraints. Journal of Petrology, 65, article egae105. <https://doi.org/10.1093/petrology/egae105>

Simandl, G.J., Mackay, D.A.R., Ma, X., Luck, P., Gravel, J., and Akam, C., 2017. The direct indicator mineral concept and QEMSCAN® applied to exploration for carbonatite and carbonatite-related ore deposits. In: Indicator Minerals in Till and Stream Sediments of the Canadian Cordillera, Ferbey, T., Plouffe, A. and Hickin, A.S., (Eds.), Geological Association of Canada, Special Paper Volume 50 and Mineralogical Association of Canada, Topics in Mineral Sciences Volume 47, pp. 175-190.

Simony, P.S., Ghent, E.D., Craw, D., and Mitchell, W., 1980. Structural and metamorphic evolution of the northeast flank of the Shuswap complex, southern Canoe River area, British Columbia. In: Cordilleran Metamorphic Core Complexes, Crittenden, M.D., Coney, P.J., and Davis, G.H., (Eds.), Geological Society of America, Memoir 153, pp. 445-461.

Song, W.L., Xu, C., Veksler, I.V., and Kynicky, J., 2016. Experimental study of REE, Ba, Sr, Mo and W partitioning between carbonatitic melt and aqueous fluid with implications for rare metal mineralization. Contributions to Mineralogy and Petrology, 171, 1-12.

Stacey, J.S., and Kramers, J.D., 1975. Approximation of terrestrial lead isotopic evolution by a two-stage model. Earth and Planetary Science Letters, 26, 207-221.

Stracke, A., 2012. Earth's heterogeneous mantle: a product of convection-driven interaction between crust and mantle. Chemical Geology, 330-331, 274-299.

Stracke, A., Hofmann, A.W., and Hart, S.R., 2005. FOZO, HIMU, and the rest of the mantle zoo. Geochemistry, Geophysics, Geosystems, 6, article Q05007. <https://doi.org/10.1029/2004GC000824>

Tatsumoto, M., Knight, R.J., and Allègre, C.J., 1973. Time differences in the formation of meteorites as determined from the ratio of lead-207 to lead-206. Science, 180, 1270-1283.

Thompson, R.I., Glombick, P., Erdmer, P., Heaman, L.M., Lemieux, Y., and Daughtry, K.L., 2006. Evolution of the ancestral Pacific margin, southern Canadian Cordillera: Insights from new geologic maps. In: Paleozoic Evolution and Metallogeny of Pericratonic Terranes at the Ancient Pacific Margin of North America, Canadian and Alaskan Cordillera, Colpron, M. and Nelson, J.L., (Eds.), Geological Association of Canada, Special Paper 45, pp. 433-482.

Trofanenko, J., Williams-Jones, A.E., Simandl, G.J., and Migdisov, A.A., 2016. The nature and origin of the REE mineralization in the Wicheeda carbonatite, British Columbia, Canada. Economic Geology, 111, 199-223.

Wheeler, J.O., and Fox, P.E., 1964. Geology, Big Bend, Seymour Arm, east half, British Columbia. Geological Survey of Canada, Preliminary Map, 12-1964, 1:253,440 scale. <https://doi.org/10.4095/108714>

White, G.P.E., 1982. Notes on carbonatites in central British Columbia. In: Geological Fieldwork 1981. British Columbia Ministry of Energy, Mines and Petroleum Resources, British Columbia Geological Survey Paper 1982-01, pp. 68-69.

Wood, B.J., Nielsen, S.G., Rehkämper, M., and Halliday, A.N., 2008. The effects of core formation on the Pb- and Tl- isotopic composition of the silicate Earth. Earth and Planetary Science Letters, 269, 325-335.

Woolley, A.R., and Kempe, D.R.C., 1989. Carbonatites: nomenclature, average chemical compositions, and element distribution. In: Carbonatites: Genesis and Evolution, Bell, K. (Ed.), Unwin Hyman, London, United Kingdom, pp. 1-14.

Xu, C., Kynicky, J., Chakhmouradian, A.R., Qi, L., and Song, W., 2010. A unique Mo deposit associated with carbonatites in the Qinling orogenic belt, central China. Lithos, 118, 50-60.

Ya'acoby, A., 2014. The petrology and petrogenesis of the Ren carbonatite sill and fenites, southeastern British Columbia, Canada. Unpublished M.Sc. thesis, The University of British Columbia, Canada, 463 p.

Yaxley, G.M., Anenburg, M., and Timmerman, S., (Eds.), 2021. Carbonatites. Elements, 17, 307-344.